HHS Public Access

Author manuscript

Matrix Biol. Author manuscript; available in PMC 2024 August 01.

Published in final edited form as:

Matrix Biol. 2023 August ; 121: 149–166. doi:10.1016/j.matbio.2023.06.007.

TSG6 hyaluronan matrix remodeling dampens the inflammatory response during colitis

Nansy Albtoush[1,4], **Kimberly A. Queisser**[1,4], **Ash Zawerton**[4], **Mark E. Lauer**[5,†], **Ellen J. Beswick**[6], **Aaron C Petrey**[1,2,3,4]

[1]University of Utah Molecular Medicine Program, Salt Lake City, Utah, 84112

[2]Department of Pathology, University of Utah School of Medicine, Salt Lake City, Utah, 84132

[3]Division of Gastroenterology, Department of Internal Medicine, University of Utah, Salt Lake City, Utah, USA

[4]Lerner Research Institute, Department of Inflammation & Immunity, Cleveland Clinic, Cleveland, OH 44195, USA

[5]Lerner Research Institute, Department of Biomedical Engineering, Cleveland Clinic, Cleveland, OH 44195, USA

[6]Division of Gastroenterology, Department of Internal Medicine, University of Kentucky, Lexington, KY, United States.

Abstract

In response to tissue injury, changes in the extracellular matrix (ECM) can directly affect the inflammatory response and contribute to disease progression or resolution. During inflammation, the glycosaminoglycan hyaluronan (HA) becomes modified by tumor necrosis factor stimulated gene-6 (TSG6). TSG6 covalently transfers heavy chain (HC) proteins from inter-α-trypsin inhibitor (IαI) to HA in a transesterification reaction and is to date is the only known HC-transferase. By modifying the HA matrix, TSG6 generates HC:HA complexes that are implicated in mediating both protective and pathological responses. Inflammatory bowel disease (IBD) is a lifelong chronic disorder with well-described remodeling of the ECM and increased mononuclear leukocyte influx into the intestinal mucosa. Deposition of HC:HA matrices is an early event in inflamed gut tissue that precedes and promotes leukocyte infiltration. However, the mechanisms by which TSG6 contributes to intestinal inflammation are not well understood. The aim of our

Address correspondence to: Aaron C. Petrey, Assistant Professor of Microbiology & Immunology, University of Utah Health Sciences Center, Eccles Institute of Human Genetics, 15 North 2030 East, Bldg 533, Suite 4250A, Salt Lake City, Utah 84112, (801) 213-2064 (phone), (801) 585-0701 (fax), aaron.petrey@u2m2.utah.edu.

†Deceased

AUTHOR CONTRIBUTIONS

N.A. designed the research, performed experiments, analyzed results, and authored the paper. K.Q designed the research, performed experiments, analyzed results A.Z. performed experiments. M.E.L. designed the research and analyzed results. A.C.P designed the research, performed experiments, analyzed results, and authored the paper.

Conflict-of-interest disclosure: The authors declare no competing financial interests.

study was to understand how the TSG6 and its enzymatic activity contributes to the inflammatory response in colitis. Our findings indicate that inflamed tissues of IBD patients show an elevated level of TSG6 and increased HC deposition and that levels of HA strongly associate with TSG6 levels in patient colon tissue specimens. Additionally, we observed that mice lacking TSG6 are more vulnerable to acute colitis and exhibit an aggravated macrophage-associated mucosal immune response characterized by elevated pro-inflammatory cytokines and chemokines and diminished anti-inflammatory mediators including IL-10. Surprisingly, along with significantly increased levels of inflammation in the absence of TSG6, tissue HA levels in mice were found to be significantly reduced and disorganized, absent of typical “HA-cable” structures. Inhibition of TSG6 HC-transferase activity leads to a loss of cell surface HA and leukocyte adhesion, indicating that the enzymatic functions of TSG6 are a major contributor to stability of the HA ECM during inflammation. Finally, using biochemically generated HC:HA matrices derived by TSG6, we show that HC:HA complexes can attenuate the inflammatory response of activated monocytes. In conclusion, our data suggests that TSG6 exerts a tissue-protective, anti-inflammatory effect via the generation of HC:HA complexes that become dysregulated in IBD.

Keywords

Extracellular matrix; Hyaluronan; TSG6; IBD; Colitis

INTRODUCTION

The extracellular matrix (ECM) functions as a physical scaffold for cells that also plays a crucial role in regulating several properties of cellular behavior including differentiation, signaling, adhesion. The ECM is a diverse network of molecules including proteins, proteoglycans, and glycosaminoglycans (GAGs) which interact with cell surface receptors to influence cellular function. In response to inflammatory cytokines, the ECM undergoes alterations of its composition, which includes degradation of the ECM by proteases, but also increased deposition ECM molecules. The ECM of inflamed tissues directly participates in inflammation by shaping the immune response of infiltrating immune cells by modulating cell activation and recruitment.

Hyaluronan (HA) is a crucial constituent within extracellular matrices and plays a significant role in intestinal tissue homeostasis[1]. HA is produced at the plasma membrane by hyaluronan synthase enzymes (HAS1–3) and is released into the ECM as a linear polysaccharide [2]. Under conditions of homeostasis, HA is typically observed as a high-molecular weight, unbranched repeating disaccharide polymer of glucuronic acid (GlcA) and N-acetyl glucosamine $[GlcNAc(\beta1–4)GlcA(\beta1–3)]_n$. A unique property of HA from other GAGs is that during development, tissue injury, inflammation, and possibly other settings, heavy chain proteins (HCs) from the proteoglycan inter-α-inhibitor (IαI) can be covalently transferred onto HA polymers and result in a HC:HA complex with distinct properties from unmodified HA[3–5]. IαI is assembled in the Golgi Apparatus in a multi-step enzymatic process that has not been fully elucidated and the liver is believed to be the major source of circulating IαI. Unlike other proteoglycans, IαI consists of at least two proteins joined to one GAG, where bikunin and one or more HCs that are

all joined to the same chondroitin sulfate (CS) polymer. There is significant homology between the individual HCs, and HC1–3 all possess a conserved C-terminal processing site required for ester-linkage to the CS attached to bikunin during biosynthesis in the Golgi. Both IαI (defined as a complex of bikunin-CS-HC1-HC2) and pre-αI (PαI) (defined as the complex of bikunin-CS-HC3) are constitutively present at high levels in circulation. Covalent modification of HA is catalyzed by tumor necrosis factor-stimulated gene 6 (TSG6), and to date is the only known enzyme with HC transferase activity to be described. This TSG6-mediated process drastically remodels HA into large “cable-like” structures that become adhesive for leukocyte:ECM interactions and are associated with several disease pathologies ranging from cancer, arthritis, asthma, and inflammatory bowel disease (IBD) [6–18].

IBD is a chronic disorder in which inflammatory leukocyte influx leads to unabated destruction of intestinal tissues. The origin of IBD is complex where a combination of viral, microbiological, and environmental factors perpetuate immuno-regulatory dysfunction in genetically susceptible individuals[19, 20]. Pathological infiltration of leukocytes into mucosal and submucosa and alterations in mucosal smooth muscle cell ECM are among the clinical manifestations of IBD. Ulcerative colitis (UC) and Crohn’s disease (CD) are the two primary subtypes of IBD, with similar symptoms but distinct clinical presentations[21, 22]. Greater than 160 IBD-associated genetic risk loci have been identified, one being the HC3 subunit of the IαI family[23, 24]. However, the specific biological functions of individual HCs and how they alter ECM composition or regulate cell behavior are not well understood and is an emerging area of study. All mucosal tissues contain homeostatic leukocyte populations which have a surveillance function maintaining tissue homeostasis and health. During IBD, affected intestinal tissue show hallmarks of an increased proportion of immune cells and leukocytes infiltrating into the inflamed submucosa become activated where they contribute to ECM remodeling and tissue destruction characteristic of IBD [25, 26]. Increased deposition of HA within the inflamed colon has been observed in IBD patient colon tissues and colitis-induced vascular leakage brings IαI from circulation in contact with tissue HA, providing a scenario in which the transferase activity of TSG6 converts HA to HC:HA matrices [27, 28]. Several studies of colitis models have demonstrated that HC:HA plays an important role in regulating leukocyte infiltration into the intestine and suggest that HC:HA matrices can directly influence the outcome of inflammatory challenge [16, 29]. Inflammation-associated HA production has been suggested as a potential therapeutic option in many diseases, however pharmacological inhibition of HA in a murine model of colitis results in exacerbated disease, supporting a possible anti-inflammatory role for HA or HC:HA in the colon [30].

A growing body of evidence suggests that TSG6 primarily exhibits potent anti-inflammatory effects as demonstrated in several murine models of inflammatory disease ranging from pulmonary inflammation, rheumatoid arthritis, pancreatitis, asthma, macular degeneration, and colitis[3, 4]. However, serum levels of HC:HA (the enzymatic product of TSG6 activity) shows a strong association with serum levels of TNF-α and endoscopic disease activity in patients with IBD[31] and several lines of evidence implicate the activity of TSG6 as an inflammation-induced regulator of leukocyte adhesion to the extracellular matrix. Given that TSG6 may play roles in both initiation and resolution of inflammation in IBD, in the present

study, we examined the role of TSG6-mediated modification of HA in the pathology of human IBD patients and mice subject to experimental model of colitis. Our data shows that TSG6 protein and activity is increased in IBD patient cells and tissues, and that deposition of HC1 and HC3, but not HC2 correlates with the inflammatory response in IBD. Loss of TSG6 in mice leads to increased tissue destruction and inflammation in a dextran sodium sulfate (DSS)-induced model of colitis along with elevated macrophage infiltration, and a significantly increased inflammatory response. Furthermore, we provide evidence that HC:HA matrices themselves can act as an immunomodulator of activated monocytes by dampening the pro-inflammatory immune response.

RESULTS

TSG6 levels are increased in colonic tissue from IBD patients

As we and other researchers have documented, HC:HA matrices which result from TSG6 activity are elevated in the intestinal tissues of both IBD patients and mice challenged with experimental colitis [14–18]. However, little is known about TSG6 expression, localization, and steady-state levels in intestinal tissues under conditions of health and disease. Therefore, we examined tissues from a cohort of patients (Table 1) with active inflammatory disease (15 CD, 15 UC) and non-inflamed non-IBD controls (15 ND) using a combination of western blot, qRT-PCR, and immunohistochemistry. Significantly increased protein (Fig 1A, 1B, S1A) and transcript levels (Fig 1C, S1B) of TSG6 were observed in both forms of IBD as compared to non-IBD control tissue specimens. However, to our surprise, we observed a low level of basal TSG6 protein and mRNA expression in non-diseased tissue specimens that was further confirmed by immunostaining (Fig 1D). Immunohistochemical analysis of colon tissue revealed that in non-IBD tissues, the majority of TSG6 protein detectable is present within epithelial cells at the base of the colonic crypts. By contrast, in tissues isolated from both UC and CD patients, TSG6 is present at increased levels within crypts, throughout the mucosal layer, and also present within regions of immune infiltrate in mucosal and submucosal tissues. These data suggest that TSG6 is present in the mucosal layer of non-IBD intestinal tissues and increased at the mRNA and protein level in IBD appears similar between disease subtypes.

Pathological Distribution of Inter-α inhibitor Heavy Chains in IBD Intestinal Tissues

The dysregulation of the ECM is closely linked to the inflammatory processes of IBD, and has functional and clinically relevant effects upon immune and non-immune cells during the course of disease development. Inflammation triggers the infiltration of immune cells into submucosal tissues, which in turn initiates a cycle of ECM degradation and synthesis that appears similar in both CD and UC and reflect the presence and degree of inflammation. In areas of inflamed submucosa, HC:HA levels have been observed to be higher than in non-inflamed regions of the same IBD patient [15, 16]. Previous studies relied upon an antibody specific for IαI that recognized all HCs and bikunin, and was therefore unable to discriminate between components of IαI. Although the presence of HA and HC:HA in serum and tissues from IBD patients as well as mice subject to experimental colitis has been described[14–17, 31, 32], the composition of specific HCs associated with HA in IBD is not known. Therefore, we examined submucosal colon tissue from either non-IBD

control (ND), UC, or CD patients with HC specific antibodies using standard IHC methods. Figure 2 depicts representative sections derived from surgical specimens removed from IBD or non-IBD control patients that are labeled with antibodies specific to individual HCs. The submucosa is a loose, vascularized connective tissue and a clear qualitative difference is observed in submucosal HC deposition in IBD patient tissue when compared with controls [15, 16] HC1 staining in control (ND) tissue is detected in the blood vessels of the submucosa as expected, as IαI circulates at high levels in serum (Fig 2A). By contrast, in both forms of IBD, HC1 is present in the ECM surrounding submucosal smooth muscle cells and connective tissue around the blood vessels having the greatest density within regions of robust leukocyte infiltration (Fig 2A). HC2 distribution demonstrated a contrasting staining pattern within the submucosa when compared with HC1. While HC1 was detected within both vessels and in the submucosal matrix, HC2 was predominantly detected in the blood vessels, and was virtually absent from the submucosal smooth muscle in both IBD and non-IBD tissues (Fig 2B). Detection of HC3 in IBD tissues (Fig 2C) was remarkably similar to that of HC1 with pronounced deposition in and around blood vessels, dense regions of leukocyte infiltration, and within the matrix surrounding submucosal smooth muscle cells in IBD tissues, whereas relatively little HC3 was detectable in control specimens.

Although prior studies have demonstrated co-localization of HCs with HA in IBD which implies the presence of HCs bound to HA, intact IαI or free HCs could be bathing the inflamed colon tissue from serum exudates. Given that ECM degradation is well-described in IBD, we next sought to obtain biochemical evidence to determine the relative abundance of IαI, HCs associated with HA, and HA-free HCs by analyzing colon tissue homogenates from non-IBD and IBD with a pan-IαI antibody (Fig 2D). The presence of HC:HA (of extremely high molecular mass at the top of the gel) was either present at very low levels or undetectable in non-IBD control specimens and found to be increased in IBD tissues by comparison. IαI (250 kDa, with two HCs) was present in all patient tissues and appears increased in IBD tissues, and likely derived from serum exudates from bleeding. To our surprise, free HCs (~75kDa) were observed in both non-IBD and IBD tissues alike, and confirmed by using a HC1-specific antibody to be present at significantly higher levels in both forms of IBD compared with non-IBD controls (Fig 2E).

TSG6 Deficiency Results in Increased Susceptibility to Colitis

HA deposition is a well-described pathological finding in tissues of patients with IBD and is recapitulated in murine experimental models of colitis. Importantly, deposition or remodeling of HA is known to regulate the early stages of inflammation in the DSS-induced model of acute colitis [14–18]. Based on this, we hypothesized that the absence of HC-transfer to HA by TSG6 would therefore alter disease progression. DSS-induced colitis in mice is characterized by a concentration- and time-dependent development of symptoms. DSS treatment weakens the epithelial barrier, allowing bacterial invasion which leads to acute colitis[33]. In order to assess the effect of TSG6 deficiency, we induced acute colitis with the addition of 2.5% DSS in the drinking water TSG6 KO and control WT mice, and monitored disease progression over 7 days. The loss of TSG6 resulted in a faster and more severe disease, as evidenced by increased overall weight loss (Fig 3A–B). Using a disease activity index (DAI) to monitor mice for outward symptoms of disease activity

on a daily basis, we found that TSG6 null mice experienced more severe symptoms (Fig 3C) compared to control mice (n=10 each). Morphological assessment of colon tissue showed no statistically significant differences in epithelial crypt structure, mucosal area, or submucosal area between TSG6 KO mice when compared with controls (supplemental Figure 2A–B). Following induction of colitis, histological staining of rectal sections on day 7 reveal increased intestinal damage demonstrated by destruction of the epithelial layer, loss of colonic crypt morphology, increased vascularization, swelling of submucosal tissue, and elevated inflammatory cell infiltration in KO mice as compared with controls (Fig 3D–E, supplemental Figure 3). Shortening of the colon is a common indicator of colitic disease severity and loss of TSG6 results in significantly reduced colon length compared with control mice (Fig 3F).

Loss of TSG6 Augments the Mucosal Immune Response

Based on the observation that TSG6 null mice exhibit increased parameters of disease when subject to DSS-induced colitis, we next investigated whether loss of TSG6 altered levels of inflammatory cytokines and immune cell recruitment, key mediators underlying the pathobiology colitis. To identify specific molecules mediating exacerbated disease activity in TSG6 KO mice during experimental colitis, we analyzed the levels of 32 different cytokines and chemokines in plasma from unchallenged and DSS-challenged mice and mice on day 7 treatment. While no differences were observed in plasma from WT or KO mice at baseline, by day 7 of DSS we observed statistically significant (*P at least < 0.05*) differences in levels of 7 pro-inflammatory mediators in TSG6-null mice as compared with WT controls including IL-12p70 (8.6-fold increased, *P<0.001),* IFNγ (2.6-fold increased, *P<0.05*), TNF-α (5.5-fold increased, *P<0.01*), IL-6 (4.3 fold increased, *P<0.01*), MCP-1 (7.8 fold increased, *P<0.001*), M-CSF (4.2 fold increased, *P<0.05*), and RANTES (4.9 fold increased, *P<0.01*). Further, cytokines with known anti-inflammatory roles in colitis including G-CSF (3.2-fold decreased, *P<0.001*) which induces M2-like macrophage responses in colitis [34], and IL-10 (4.4 fold decreased, *P<0.01*) which has an essential role in maintaining intestinal homeostasis [35], were significantly decreased on day 7 of DSS in TSG6 KO mice compared with controls (Fig 4A).

Prior literature from our lab and others has shown that dysregulation of HA in murine colitis is associated with increased levels of TNF-α, and that HA fragmentation can induce expression of and IL-6, MCP-1 and RANTES in a CD44 dependent manner [18, 32, 36, 37]. We therefore analyzed colon tissue homogenates by ELISA for tissue levels of pro-inflammatory mediators TNF-α, IL-6, MCP-1 and RANTES as well as anti-inflammatory regulators of colitis G-CSF and IL-10 (Fig 4B). Consistent with our observations in plasma, TNF-α (*P<0.01),* IL-6 (*P<0.01),* MCP-1 (*P<0.01),* and RANTES (*P<0.01),* were present at increased levels while G-CSF (*P<0.01),* and IL-10 (*P<0.05),* were decreased in DSS-treated TSG6 null mice as compared with controls with no significant present levels between genotypes in the absence of DSS treatment.

Given the finding that macrophage- and dendritic cell- derived cytokines (TNF-α, IL-6, and IL12p70) and monocyte chemo-attractants (MCP-1, RANTES, and M-CSF) were present at high levels in systemic circulation and/or inflamed colon tissue, we next assessed

macrophage infiltration using immunohistochemical staining of rectal colon sections from mice. Analysis of F4/80+ macrophages present within mucosal and submucosal regions of WT and TSG6 KO mice showed no significant differences between unchallenged animals. By day 7 of DSS however, levels of F4/80+ macrophages present in tissue appear robustly increased in TSG6 KO mice compared with controls (Figs 4C, D).

TSG6 Modulates Tissue HA Quantity and Organization in Colitis

Alteration of the ECM in intestinal inflammation (degradation and de novo synthesis) is appreciated as an active participant in IBD pathobiology. Increased HA deposition is well described in IBD tissues and the size and composition of HA within the ECM is known to regulate cell behavior during homeostasis and inflammation. We were then were interested in the expression of the three HAS isoforms and HA size profile in colon tissue from IBD patients. Real-time qPCR data showed significant increased expression of *HAS2* and *HAS3* in tissues from IBD patients compared with healthy controls (Fig 5A, S1C). Subsequently, we examined the HA size distribution of the tissue samples by isolating GAGs from colon specimens and analyzing their size distribution through agarose gel electrophoresis (Fig 5B) using the same specimens.

We found that IBD tissues had elevated levels of HA, as evidenced by the increased amount of dark-stained material across all polydisperse molecular weights, indicating an overall increase in HA content in IBD tissues compared to non-IBD controls. We then quantified HA isolated from tissue by competitive ELISA-like assay by first analyzing total HA (Fig 5C) and further size fractionated isolated HA to determine the relative abundance of low-molecular weight HA fragments (Fig 5D), revealing that HA levels are broadly increased as well at low-molecular weight ranges indicative of HA degradation in IBD. Next, we sought to determine whether the protein level of TSG6 is associated with tissue HA in human colon specimens. This analysis revealed a significant positive correlation between TSG6 and total HA (Fig 5E) in human colon tissues but found no association between TSG6 and low-molecular weight HA, suggesting that TSG6 expression may contribute to the regulation of HA size and stability.

We next examined how loss of TSG6 in mice affected HA levels, HA synthase expression, and HA tissue distribution under basal conditions and during DSS-induced colitis. Analysis of *HAS* gene expression in colon tissue is consistent with prior studies showing *HAS2* is the predominant enzyme expressed in the murine colon[30], and showed no significant differences in *HAS1–3* gene expression between TSG6 KO and WT mice under either inflammatory challenge (Fig 5F) or basal conditions (data not shown). To investigate how loss of TSG6 affected HA distribution during colitis we measured total HA levels and stained histological sections for HA in rectal colon tissue. After 7 days of DSS-treatment, total HA levels in colon tissue was significantly reduced in TSG6 null mice relative to controls (Fig 5G), but showed no difference in unchallenged animals. As depicted in Fig 5H, the level and distribution of HA within all colon layers is comparable between TSG6 KO mice and wildtype controls. Treatment with DSS significantly increased HA accumulation in mucosal and submucosal colon tissue (Fig 5H). Notably, HA deposition in the colons of TSG6 KO mice appeared reduced by trend in agreement with quantitative measures (Fig

5G), and further appeared to be more diffusely distributed and lacking the characteristic "cable-like" structure formed by HC-modification of HA commonly described in prior studies [14, 16, 18]. Taken together, these data indicate that TSG6 plays a role in regulating tissue HA quantity and organization during acute colitis.

TSG6 Activity is Required to Retain and Organize Leukocyte Adhesive HA to the Cell Surface

TSG6 expression is crucial in the differentiation of fibroblasts into myofibroblasts by facilitating the formation and arrangement of a pericellular matrix rich in HA[38]. The importance of TSG6 in matrix organization is further supported by the role of the HC:HA matrix during formation of the cumulus cell oocyte complex where other matrix proteins, such as pentraxin 3, bind to HC-HA and stabilize expansion of the ECM, which is required for ovulation and fertilization in virtually all mammals [39–41]. Based on the observation that loss of TSG6 impacted the localization, organization, and quantity of HA during murine colitis, we next sought to test whether the enzymatic activity of TSG6 could directly regulate HA levels at the cell surface in response to inflammatory stimuli. As a first step, we screened five monoclonal antibodies (designated NG2, NG3, NG4, NG5, and NG8)[42] developed against recombinant murine TSG6 for neutralizing activity using a TSG6 HC-transfer assay [43]. Using serum as a source of IαI, recombinant hTSG6, and HA14 (an HA oligo 14 monosaccharides long which acts as an irreversible acceptor of HCs [43]), we found that HC transfer can be completely inhibited by clone NG4, but saw no such inhibition by either clone NG5 (Supplemental Figure 4 A,B) or other mAbs tested (data not shown).

Treatment of cells with the viral mimic polyinosinic acid:polycytidylic acid (poly(I:C)) in vitro increases cell surface HA and forms leukocyte-adhesive "cable-like" HC-HA structures [14–17]. We next sought to determine how inhibition of TSG6 impacted cell-surface HA matrix by measuring the quantity of HA in either the cell layer or secreted into the culture media of human mucosal smooth muscle cells (M-SMCs) isolated from IBD and non-IBD patient tissues (Fig 6A, B). Consistent with prior reports, comparison of HA levels shows that while HA is present in the cell layer, the vast majority is secreted into the media. To our surprise, unstimulated M-SMCs from IBD patients exhibit an overall increase in cell-layer HA (3.24-fold greater, $p<0.001$) as compared with non-IBD cells (Fig 6A). Treatment with poly(I:C) (100 μg/ml) for 18 hours leads to a significant increase in levels of cell-layer and media HA as expected. However, co-incubation with NG4, but not NG5, abrogates this increase in layer HA and led to an increase in media HA levels in both non-IBD and IBD cells. Treatment with either NG4 or NG5 mAbs alone showed no effect on HA synthesis (Fig 6A,B) or on cell viability (Supplemental Figure 5). Antibody-neutralization of IαI is known to prevent formation of HC:HA cable structures, and we next determined whether neutralization of TSG6 activity was sufficient to alter the remodeling of HA at the cell surface. Primary M-SMCs were cultured with medium, medium supplemented with poly(I:C), or co-treated with poly(I:C) and either anti-TSG6 mAb NG4 or mAb NG5. Organization of cell-surface HA was examined using a highly specific HA-binding probe and the M-SMC plasma membrane was detected using a monoclonal antibody to the HA-receptor CD44. Cells treated with medium alone possess a low amount of HA which is distributed as an uneven pericellular matrix (Fig 6C). In cells stimulated with poly(I:C), HA

is remodeled into HC:HA complexes with “cable-like” appearances (Fig 6, arrows) that are up to several cells in length and HA is also observed as increased coats on the cell surface. The addition of NG4 (a mAb which inhibits TSG6) to poly(I:C)-stimulated M-SMCs has no effect on the HA pericellular matrix but HC:HA structures are no longer detected. By contrast, addition of NG5 which binds TSG6 but does not inhibit HC transfer displayed showed no effect on the organization of HA with poly(I:C)-stimulated cells.

Inhibition of TSG6 HC-transferase Activity Reduces Leukocyte Adhesion

Our previous studies demonstrated that destruction of HC:HA cables by either the protease thrombin or by platelet hyaluronidase-2 directly inhibits leukocyte adhesion to cell surfaces [17, 18]. Therefore, we asked whether mAbs NG4 (which inhibits TSG6 activity) or NG5 (which does not inhibit TSG6) (Supplemental Figure 4) could affect immune cell adhesion to M-SMCs stimulated with poly(I:C). Cells were cultured with media alone, with individual mAbs (with no effect on viability Supplemental Figure 4), or treated with poly(I:C) with or without either NG4 or NG5. After overnight treatment to induce HC:HA, adhesion of peripheral blood mononuclear cells (PBMCs) was examined. Poly(I:C) treatment of M-SMCs enhances adhesion of PBMCs, when compared to either mAb alone or control treatment (Fig 6D, Supplemental Figure 6). Simultaneous treatment of cells with poly(I:C) and NG4 attenuated PBMC adhesion to M-SMCs as compared with poly(I:C) alone or poly(I:C) with NG5, suggesting that increased adhesion depends on TSG6 transferase activity. As a control to demonstrate the degree of HA-dependent adhesion, M-SMCs were pretreated with hyaluronidase to remove HC:HA from the cell surface prior to addition of PBMCs, which led to significantly reduced leukocyte adhesion.

Monocyte Interaction with HC:HA Matrices Attenuates Inflammatory Responses

TSG6 is known to alter the inflammatory response by biasing macrophage responses toward an anti-inflammatory M2-like phenotype in murine and *in vitro* models [44–49]. Under *in vitro* contexts of LPS-activation, RAW264.7-differentiated macrophages on an immobilized HC:HA matrix demonstrate increased expression of M2 markers including IL-10, and reduced expression of M1 markers such as IL-12 and TNF-α [44]. Given the high levels of TSG6 (Fig 1) and HCs (Fig 2) in the submucosal region of inflamed IBD colons, and that naïve leukocytes specifically bind to HC:HA produced by M-SMCs isolated from IBD patient tissues[14, 15, 17], we speculated that HC:HA may shape the inflammatory response of tissue infiltrating monocytes. To test this, we covalently immobilized either HA or HC:HA using carbodiimide coupling chemistry [44, 50]. We seeded U937 monocytic cells in wells with or without HA, HC:HA, carbodiimide control reagents, or control-reagent treated surfaces in the presence or absence of poly(I:C) or LPS. We then used a combination of qPCR and ELISA to measure downstream mRNA expression and secretion of MCP-1, a chemokine we found to be significantly increased in colitic TSG6 null mice compared to controls (Fig 4A, B, S7A, S7B). We found that treatment of monocytes seeded on immobilized control with either poly(I:C) or LPS significantly induces MCP-1 mRNA and secretion into the media as compared with untreated cells. Poly(I:C) or LPS-activated monocytes on immobilized HA or with control reagents showed similar levels of MCP-1 expression and secretion. However, monocytes treated with either agonist which were seeded on a HC:HA matrix show significantly reduced levels of MCP-1 mRNA and MCP-1

protein secreted into the media compared with those treated in the presence of HA or controls (Fig 7A, B, S7A, S7B).

The transcription factor IRF5 has a well described role in directing monocytes toward an inflammatory phenotype by promoting differentiation of Ly6C^{hi} monocytes into M1-like macrophages and is known to transcriptionally activate IL-12p70, TNF-α, MCP-1, and down-regulate IL-10, all of which are dysregulated in TSG6-null colitic mice (Fig 4A) [51, 52]. Given that IRF5 deficiency in mice exacerbates colitis via an inflammatory macrophage phenotype [53], and that HC:HA down-regulates IRF5 in LPS-activated macrophages [44], we asked whether HC:HA might also regulate expression of IRF5 in monocytes. Monocytes seeded on HC:HA show reduced basal IRF5 levels as compared to monocytes seeded on either HA or immobilization control. Treatment with LPS induces a greatly induces in IRF5 protein expression in monocytes seeded on HA, but not with monocytes seeded on HC:HA (Fig 7C). Similar to observations in LPS-activated macrophages, HC:HA matrices generated by TSG6 are capable of down-regulating inflammatory genes via IRF5 in activated monocytes.

We next sought to determine whether alterations in monocyte functional responses (e.g. MCP-1 expression and secretion) corresponded with known markers of inflammatory or anti-inflammatory monocyte populations. We next compared the mean fluorescence intensity (MFI) of two monocyte/macrophage markers: CD38, a marker associated with inflammatory monocytes and macrophages with that of CD163, a marker strongly induced by anti-inflammatory mediators. Unstimulated monocytes showed no significant changes in cell-surface expression of either CD38 or CD163 after culture with immobilization controls, HA, or HC:HA matrices (Fig 7D, S7C, S7D). However, U937 monocytes activated with LPS showed a significant increase in CD38 expression compared to unstimulated controls which was attenuated in cells cultured on HC:HA. Cell surface expression of CD163 in resting monocytes trended towards an increase that was not statistically significant on HC:HA, while LPS-activated monocytes cultured on HC:HA, but not control or HA, showed a statistically significant 1.9-fold increase in CD163 expression. Based on these data, we next asked we asked whether CD163+ cells of the monocyte/macrophage lineage co-localized with regions of HC:HA. Immunostaining of human colon tissue sections revealed CD163+ cells distributed throughout the submucosa of ND tissues adjacent to HCs of IαI within the ECM. Examination of inflamed IBD tissue showed a significant increase in tissue HC, along with abundant CD163+ cells entrapped within the HC ECM (Fig 7E). As expected with the inflammatory process where HC and CD163+ cells become increased in tissue, HCs showed significant levels of colocalization (Pearson correlation coefficient, 0.59) in IBD tissue compared with control (Pearson = 0.34). Collectively, these data suggest HC:HA matrices generated by TSG6 are capable of recruiting and exerting an anti-inflammatory on activated monocytes.

Discussion

Our study employed a combination of IBD surgical specimens, murine models, human colon tissue derived primary cells, and biochemical assays to present evidence that TSG6's enzymatic activity has an anti-inflammatory role in colitis. We found that TSG6 levels are

increased at both the protein and mRNA level in colon tissue from patients with active disease of both forms of IBD, and localized within mucosal and submucosal regions of immune infiltrate. Our findings also reveal that the deposition of HCs derived from IαI is not uniform across different HCs, with HC1 and HC3 (but not HC2) present in increased levels in IBD patient tissues. Using a model of acute colitis, our findings demonstrate that TSG6 deficient mice are more vulnerable to tissue damage and inflammation driven by an aggravated mucosal inflammatory response. Our data from human and murine tissue paired with biochemical experiments in primary cells using a TSG6-inhibiting antibody suggests that the activity of TSG6 plays a role stabilizing the quantity, size, and tissue organization of HA and has a direct effect on leukocyte adhesion. Finally, using biochemical methods we show that monocyte interaction with HC:HA exerts a protective effect on activated monocytes by downregulating pro-inflammatory pathways. Together, our data indicates that the enzymatic activity of TSG6 plays an important role generating HC:HA matrices and thereby shaping the immune response by repressing inflammatory pathways (Figure 8).

Previous studies described TSG6 as an anti-inflammatory molecule secreted by TNF-α stimulated fibroblasts identified as a member of the HA-binding link module superfamily [54, 55]. Mice deficient in TSG6 demonstrated an increased susceptibility to arthritis and enhanced inflammation, while transgenic mice overexpressing TSG6 demonstrated resistance to collagen-induced arthritis [56] [57]. Since then, beneficial effects of TSG6 treatment with either exogenous enzyme or cell-based therapies have been described in multiple murine models of inflammation ranging from arthritis, age-related macular degeneration, neurodegenerative disease, vascular injury, lung inflammation, and colitis [45–49, 57–61]. These studies have collectively demonstrated broad ranging therapeutic effects on stromal cells and immune cells including dendritic cells, monocytes, and T cells [3]. Our study builds upon observations drawn from several murine colitis models where mice treated with either recombinant TSG6, mesenchymal stem cells (MSCs) or extracellular vesicles from MSCs as source of TSG6 collectively show treatment with TSG6 reduced the severity of colitis, attenuated mucosal inflammatory response, increased levels of anti-inflammatory IL-10, and promoted a shift toward M2-like macrophage polarization. The mechanisms by which TSG6 exerts its immunomodulatory functions have been difficult to define as TSG6 interacts with an extensive array of ligands including proteoglycans, chemokines, glycosaminoglycans, and other matrix molecules. Crucially, TSG6 is the only known enzyme to catalyze the covalent modification of HA with the HCs from the IαI family of proteoglycans.

Despite evidence that TSG6 is essential for remodeling of the HA ECM, the role of HC:HA itself as a pro- or anti-inflammatory molecule is unclear. In the present study, we sought to better delineate how the HA matrix modifying activity of TSG6 to generate HC:HA contributed to the mucosal immune response. Our study's findings emphasize an essential regulatory interplay between the ECM and infiltrating monocytes mediated by TSG6. HA accumulates at the early pathological changes in the inflamed distal colon before the infiltration of inflammatory cells [16] where it supports leukocyte adhesion. Here, we show that in tissue from non-IBD patients, TSG6 is expressed at the base of mucosal epithelial cells and in patients with active IBD TSG6 is present at increased levels throughout the layers of the colon as at the level of messenger RNA and protein. Although TSG6 is seldom

expressed outside of the context of inflammation, a basal expression of TSG6 and HCs is reported in various epithelial cell types [11, 62, 63]. These findings indicate a possible role for TSG6 and HA in maintenance or regeneration of epithelial cells, where HA has been shown to induce epithelial defense mechanisms and induce wound healing [58, 64–68]. Our analysis of the submucosa of IBD patients confirmed that HC deposition increases in IBD, consistent with our previous reports using an antibody that recognized all forms of HC:HA [14, 15]. Notably, deposition of HCs 1 and 3 were increased in the submucosa of both forms of IBD compared with controls and although HC2 was present in both patient groups, the tissue localization of HC2 appears restricted exclusively to the surface of blood vessels in both IBD and non-IBD tissues. While we observed increased HC:HA in IBD patient tissues compared with controls as expected (Fig 2D, E), we also detected a significant increase in tissue HCs free from either HA or IαI in IBD patients which indicates increased matrix remodeling activity associated with IBD [69]. However, given that the source of free HC1 observed in non-IBD tissues is unknown, we cannot rule out the possibility that individual HCs may be expressed within GI tissues, perhaps by epithelial cells as in the amniotic membrane, lung, and kidney [11, 62, 63].

Using a well characterized murine model of acute colitis, we examined the contribution of TSG6 to intestinal inflammation. The murine DSS model has been used to demonstrate that HA deposition occurs early on during intestinal inflammation, often before inflammatory destruction of the distal colon [16]. We have demonstrated that TSG6 deficiency aggravates the outward signs of disease and pathological changes in the colon. Analysis of rectal sections from TSG6-null mice consistently revealed intestinal damage characterized by a broken epithelial layer, destruction of crypt structure, swelling of submucosal tissue, microvascular remodeling, and robust infiltration of inflammatory cells into damaged tissues. Loss of TSG6 resulted in a significantly increased inflammatory response, as indicated by elevated cytokine levels and increased infiltration of F4/80+ macrophages into the colon. These observations are consistent with the role of TSG6 in LPS-induced lung injury, where TSG6-null mice exhibited an enhanced inflammatory response driven by TNFα, IL-1β, IL-6, and IL-12p70, compared to wildtype controls [49]. In addition to elevated levels of pro-inflammatory molecules in TSG6 KO mice, our data revealed an unexpected and striking reduction in IL-10, which plays an essential role in maintaining mucosal homeostasis and serves as an important regulator in preventing pro-inflammatory responses. Production of IL-10 arises from a number of immune cells within the GI tract, including dendritic cells, macrophages, T-cells, and T-regulatory cells [70]. The protective functions of IL-10 are attributed to dampening over-exuberant immune responses, preventing cytokine and chemokine production and in mucosal tissues acts primarily on macrophages and T-regulatory cells. In the DSS-colitis model, IL-10 has been shown to exert its protective role by regulating a macrophage-ROS-NO axis to limit inflammation[35]. Therapeutic treatment of IBD patients with anti-TNF depends upon IL-10 signaling in macrophages, resulting in an increase in CD206+ M2-like macrophages[71].

Our experiments examining the HA content in IBD patient tissues and mice sought to determine how TSG6 affects HA homeostasis. Examination of colitic mice support a role for HAS2, and to a lesser extent, HAS3 in generation of HA in response to intestinal inflammation in agreement with prior studies[30]. We further examined the size profile

and quantity of HA isolated from IBD tissues and these are suggestive of a cycle of HA synthesis and degradation as evidenced by broadly increased quantity of HA of both high- and low-molecular weight in IBD tissues. In inflamed tissue sections from IBD patient colons and from mice subject to experimental colitis, HA is organized into delicate cable-like HC:HA structures by TSG6 [15, 17]. Mice deficient in TSG6 do not produce HC:HA complexes and show reduced deposition of pulmonary HA in response to inflammatory challenge [10]. Our own analysis of colitic mice lacking TSG6 show a quantitative reduction in HA levels isolated from colon tissues upon inflammatory challenge despite equivalent base-line levels, similar to observations in eosinophilic asthma[10]. Notably, while we also observed decreases in tissue HA, the residual HA within colonic tissues appeared disorganized and diffuse, entirely unlike the organization of HA in control mice. We provide immunohistochemical evidence that the absence of TSG6 and HC transferase activity leads to altered organization of HA within inflamed tissues.

In light of these data and that several inflammatory cytokines (such as IL-12 and MCP-1) were increased in the inflamed colon of TSG6-null mice play essential roles in monocyte recruitment, we hypothesized that loss of HC:HA matrices might alter monocyte gene expression similar to known effects on macrophages. Our *in vitro* experiments show that HC:HA, but not HA alone, exerts an anti-inflammatory effect on Poly(I:C) or LPS-stimulated U937 monocytic cells leading to reduced expression and secretion of MCP-1 and reduced surface expression of the M1-like macrophage marker CD38. Similar to other studies in which LPS-activated macrophages were exposed to HC:HA[44], our data also suggests that HC:HA may exert broad effects on monocyte functions via IRF5 and “shape” activated monocyte differentiation towards an M2-like phenotype. Consistent with this, we observed increased co-localization between the M2 marker CD163 and HC:HA in IBD tissues, where the expansion of M2-like macrophages is associated with disease[72].

Although our data may strongly support an anti-inflammatory function of TSG6 in IBD, several open questions remain. Murine studies of colitis in which TSG6 has been delivered as a treatment by several different modalities have shown beneficial effects (as reviewed here [3]), and this seems consistent with our own data that TSG6 deficiency in mice exacerbates colitis. We also observed greatly increased TSG6 levels in tissue from IBD patients with active disease which might seem to be in conflict with the findings of anti-inflammatory role of TSG6 in mice. One possible explanation involves the degradation of the HA ECM in IBD which has been well described [15, 16, 73]. Our analysis of alterations in HA size including at low-molecular weights, and the detection of HA-free HCs in IBD patient tissue specimens supports the notion that the HA matrix in IBD is disrupted even in the presence of greatly increased TSG6 levels. Degradation or destabilization of the ECM matrix by hyaluronidases, proteases, or reactive oxygen species could result in loss of tissue protective functions of HC:HA. Further, during both IBD and murine colitis, the cellular makeup of colon tissue changes dramatically during tissue inflammation, making a causal relationship between TSG6, HA deposition, and disease activity difficult. However, preclinical studies in DSS-challenged mice indicate that inhibition of HA production with 4-Methylumbelliferone (4-MU) leads to enhanced colon tissue destruction [30], and while the effects of 4-MU are not exclusive to HA as it depletes the precursor sugar-nucleotide pool for all GAGs, these data do support the tissue-protective role for HA in the gut. Given that we observed the

majority of TSG6 was localized to colonic crypts in non-IBD colon specimens while in IBD tissues TSG6 is increased throughout the epithelial layer and within the submucosal tissue including endothelial microvessels, tissue-specific TSG6 knock-outs are needed to determine epithelial vs submucosal functions. These findings are similar to reported roles of HA in the gut, where epithelial HA plays an important role in homeostasis, defense, and repair [58, 65, 67, 68, 74, 75], endothelial HA synthesis by HAS3 and vascular HC:HA aids in immune recruitment[16, 18, 30, 76].

Two limitations of our study lie in the nature of the animal model used and the systemic loss of TSG6. The murine model of DSS-induced colitis is a well-established, reproducible model of bacterially-driven intestinal inflammation but does not fully capture the complex interplay of innate and adaptive immune dysregulation of human IBD, which can be highly heterogeneous. However, the DSS-colitis model is well suited to studying the crucial role of innate immune cells including monocytes, macrophages, and neutrophils which are some of the earliest cells involved in the acute phase of disease pathogenesis and ECM remodeling. Emerging data demonstrates that HA also functions as a potent regulator of adaptive immune responses, where HA can also direct T-cells toward a Th1 phenotype [77, 78]. Our study is similar to several others of TSG6 in that we also relied upon a systemic loss of TSG6, in which both enzymatic and non-enzymatic properties of TSG6 are entirely ablated in mice. Although we sought to clarify the role of TSG6 using multiple approaches, total absence of TSG6 in our *in vivo* studies poses a few limitations on the interpretations of our data. Chiefly, we cannot clearly delineate how the specific enzymatic and ligand-binding functions of TSG6 contribute to the immune response in murine colitis. It is plausible that some of the effects observed *in vivo* could be due to the absence of TSG6 binding to chemokines, GAGs, growth factors, or other matrix proteins. For example, TSG6 interactions with CXCL8 have can prevent neutrophil migration by competing for binding of CXCL8 to GAGs on the endothelial surface [79]. Our data does not rule out the contribution of non-enzymatic anti-inflammatory functions of TSG6 beyond the scope of our study. Despite the fact that both HA and TSG6 play essential roles in tissue development, relatively little is known about the contribution of either molecule to the function of tissue resident macrophage populations which have important roles in homeostasis and remodeling and are known to express the HA receptor LYVE-1 and exhibit an M2-like phenotype [80]. While these studies provide evidence of TSG6's clear role in HC:HA matrix remodeling during inflammation, they also highlight the need for further research using catalytically inactive or tissue-specific knock-outs or TSG6 to better dissect the immunomodulatory properties of TSG6.

To date, the mechanisms by which HC:HA matrices contribute to both tissue-protective and inflammatory activities are not well understood. Altogether, these data support a model for a tissue-protective, anti-inflammatory role for TSG6 in intestinal inflammation which contributes to the monocyte/macrophage innate immune response. Our new data suggests that the HC transferase activity of TSG6 is essential for retaining HA at the cell surface, and that in addition to playing a key role in regulating leukocyte adhesion, the HC:HA matrix itself regulates the inflammatory phenotype of activated monocytes. We believe this data suggests that degradation of the HA-ECM in chronic inflammatory diseases such as IBD

leads to loss of tissue protective mechanisms regulated by TSG6. Therefore, our study may provide an unanticipated opportunity for development of novel therapeutic strategies in IBD.

MATERIALS AND METHODS

Patient surgical specimens

The Department of Anatomical Pathology at the Cleveland Clinic Foundation provided all the tissue specimens for this study. The samples were taken from surgically removed colons within two hours after surgery, and collected based on an approved Institutional Review Board protocol. The study consisted of 34 specimens from patients with IBD (17 CD, 17 UC) with active disease and 15 specimens from non-IBD controls who underwent colectomy for reasons unrelated to inflammatory enteropathies. For each subject, four specimens were collected from the same mucosal area for immunohistochemical, qRT-PCR, western blot, and ELISA. The diagnosis of all specimens was confirmed by clinical criteria, and they were of colonic origin. Non-IBD (control) tissues were obtained from histologically normal, noninflamed large bowel specimens from patients who underwent bowel resection for various reasons. The mucosal layer of each colon was dissected, washed, and cleaned by blotting with paper towels multiple times. The mucosal layer was then cut into small strips of about 0.5 cm and snap-frozen in liquid nitrogen. Specimens were age and sex matched to control for potential confounding variables.

Human Tissue Immunohistochemistry

Human colon tissue sections from both IBD and non-IBD patients were fixed with histochoice fixation (H120, Amresco, Solon, OH) and embedded in paraffin onto microscope slides. The slides were then deparaffinized. The Histology Core Facility at Cleveland Clinic Lerner Research Institute conducted all immunostaining using primary antibodies specific to TSG6 (mAb NG4) and HCs (HC1, HC2, HC3) and visualized them using either Alexa-Fluor-568 or horse-radish peroxidase conjugated secondary antibody on serial sections (where possible). Morphometric immunohistochemistry images were captured at 20× magnification using a Leica Slide Scanner SCN400 (Leica), and quantitative analysis was conducted using Image-Pro Premiere software (Media Cybernetics, Rockville, MD).

Mice

All animal experiments were conducted according to the animal welfare protocol approved by the Institutional Animal Care and Use Committee (IACUC) of Lerner Research Institute. Adult c57Bl/6 mice of both sexes were bred and housed in microisolator cages in a specific pathogen-free (SPF) environment at the LRI Biological Resource Unit. The mice had access to Teklad irradiated chow and acidified water ad libitum. Age- and gender-matched mice (groups of 5 or less per cage) were cohoused in in SPF microisolator cages the LRI Biological Resource Unit. The mice were monitored for temperature and humidity conditions, and BRU staff performed all routine husbandry. All wild-type mice (c57Bl/6J Stock number 000664) were purchased from Jackson Labs, Bar Harbor, ME, while the TSG6 null mice on a c57Bl/6J background were provided by Dr. Vincent Hascall.

DSS-Induced Colitis Model

The experimental dextran sodium sulfate-induced colitis model was conducted following described methods[18, 33]. Briefly, The mice acidified in-house water ad libitum, with or without 2.5% dextran sodium sulfate (MP Biomedicals) in water bottles. Mice were observed daily for weight changes and for outward symptoms of colitis. On days 0, 3, 5, and 7, the mice were sacrificed in accordance with approved IACUC protocols. Serum was obtained via cardiac puncture, and colons were excised and measured for length (cm) from the rectum to the cecum. The colons were fixed in molecular biology grade Histochoice (AMRESCO, Solon, OH) at ten times the tissue volume and processed by the LRI Histology Core Service Department.

Disease Activity Index

The mice that received 2.5% DSS were evaluated for parameters of colitis using a phenotypic scoring system previously reported in the literature [81]. The scoring system ranged from 0 to a maximum total of 11 points, and included the following parameters: weight change, posture, coat fur, stool texture and consistency, and rectal prolapse. Change in weight was determined by comparing each individual animal's daily weight - starting weight)/starting weight x 100, with scores assigned as follows: 0–5% (score 0), 6–10% (score 1), 11–15% (score 2), 15–20% (score 3), and >20% (score 4). Posture was evaluated as normal (score 0) or hunched (score 1). Coat fur was observed as normal (score 0) or ruffled (score 1). Stool were assessed for consistency and recorded as normal (score 0), soft (score 1), soft with blood (score 2), or liquid and bloody (score 3). Prolapse of the rectum was recorded as none (score 0), 1 mm (score 1), or 2 mm (score 2).

Histological Scoring of Colitis

Rectal sections measuring 1 cm were collected from all mice on the day of sacrifice and fixed in Histochoice for 24 hours at 25°C. After processing, 2.5 um cross-sections were stained with hematoxylin and eosin. Blinded assessments were performed using a scale that ranged from a score of 5 (histologically normal) and a score of 20 (maximum gross disease) were used evaluate tissues from all mice based on previous rating systems [18]. Integrity of the epithelial layer was evaluated by: (1) complete epithelial layer and a clearly defined crypt morphology, (2) intact epithelial layer and loss of crypt morphology, (3) breakdown of the epithelial layer and loss of crypt morphology, and (4) complete denuded epithelium and absent crypt morphology. Immune cell infiltrate is scored as: (1) absent, (2) limited, (3) moderately increased, and (4) drastic. Submucosal swelling was assessed using the muscularis mucosae layer as an upper boundary and scored as (1) no difference, (2) limited swelling, (3) moderate swelling, and (4) extreme swelling. Hyperplasia of the muscularis mucosae were measured for: (1) no difference, (2) limited, (3) moderately increased, and (4) greatly increased. Vascular remodeling and angiogenesis assessed by: changes in the size and number of microvessels as (1) no difference, (2) minor increase, (3) moderately increased, and (4) severely increased. All tissue processing, sectioning, and staining were performed by the LRI Histology Core Services Department.

Tissue Histology and Immunohistochemistry

Images were of rectal sections stained with hematoxylin and eosin were captured at 20× magnification using a Leica Slide Scanner SCN400 (Leica) using and Leica Application Suite software (Leica Corp, Buffalo Grove, IL) and tissue morphology was measured using Image ProPlus. Immunostaining was conducted to observe changes in the abundance and location of HA and F4/80+ macrophages associated with disease, using previously published protocols [24]. Briefly, tissue sections were deparaffinized using a series of solutions, including Clear-Rite 3 (2 × 3 min), Flex 100 (2 min, 1 min), Flex 95 (2 min, 1 min) (Richard Allan-Thermo Scientific, Kalamazoo, MI), and tap water. Tissue was then encircled with a Pap-Pen (Research Products International, Mt. Prospect, IL) and blocked for 30 min in 2% Fetal Bovine Serum-Hank's buffered saline (2% FBS-HBSS). Biotinylated hyaluronan binding protein (HABP) (Calbiochem-EMD Millipore, Billerica, MA), F4/80 antibody, CD163 antibody, or IαI (Dako) were diluted to 1 : 100 in 2% FBS-HBSS, was applied overnight at 4°C. The slides were washed three times in HBSS before adding streptavidin-488 (1 : 500) (Life Technologies, Grand Island, NY) in 2% FBS-HBSS for 45 minutes in the dark at 25°C. After three more washes in HBSS, the slides were mounted under cover glass with Vectashield + DAPI (Vector Labs, Burlingame, CA) and sealed with nail polish. F4/80+ macrophage infiltrates were detected using a Leica TCS SP5 II Confocal/Multi-Photon high-speed upright microscope with Acousto-Optical Beam Splitter was used to capture all images using a HCX PL APO 40X/1.25NA oil immersion objective and HyD system detector. The Leica LAS confocal software was utilized to acquire the images. Semiquantitative measurement of F4/80+ macrophages were obtained by analyzing individual images of the Z-stack using Image-Pro Plus software (Rockville, MD). Pearson's correlation coefficients were obtained by analyzing individual images (layers) of the Z-stack using Image-Pro Plus software (Media Cybernetics, Rockville, MD). Staining was performed by the Cleveland Clinic Lerner Research Institute Histology Core Facility.

Primary Cell Isolation and Culture

Human colon specimens were collected from patients who underwent surgery at the Department of Anatomical Pathology, Cleveland Clinic. As previously described[14], the mucosal layer was removed, and the lamina propria (LP) was washed using Hanks' BSS (HBSS) with 0.15% DTT (w/v) for 30 minutes, followed by washing with HBSS with 1mM EDTA for 1 hour 3x, and then 4x in HBSS (without EDTA) for 30 minutes. Rinsed LP strips were then incubated overnight in an enzyme digestion solution consisting of: collagenase, DNase (0.1 mg/ml each), penicillin (250 units/ml), streptomycin (250 μg/ml), and fungizone (0.625 μg/ml). The cells were filtered using a 10-μm cell strainer and cultured in DMEM/F-12 medium supplemented with 10% fetal bovine serum and antibiotics (penicillin, 100 units/ml; streptomycin, 100 μg/ml; fungizone, 0.25 μg/ml), and used for no greater than five passages.

Human Monocyte U937 Culture

U937 cells were acquired from American Type Culture Collection and cultured in complete RPMI, 1640 (Corning, Cellgro) supplemented with 10% fetal bovine serum (FBS) (Invitrogen), 1% penicillin/streptomycin (Cellgro) at 37°C, 5% CO2. Cells were then plated

at 5×10^5 cells/ml in fresh media for the indicated time points. To activate cells, medium was replaced with fresh media alone with Poly(I:C) treatment (100 μg/ml) or 10 ng/ml LPS (Enzo) and monocytes were incubated on control, HA, or HC:HA coated wells. After 4 h, cells were collected and analyzed for RNA or after 24 hours for protein expression and cytokine secretion into conditioned medium.

Immunofluorescent Analysis of M-SMCs

M-SMCs were cultured on ibidi glass chamber slides and allowed to grow to confluence for 2–3 days before assay [17]. Poly(I·C) treatment (100 μg/ml) was applied to M-SMCs in the presence or absence of NG4 or NG5 mAbs (500 ng/mL) 18 hours prior to the assay. Cell viability measured using a fluorescence-based live-dead assay (Ibidi, Germany) according to the manufacturer's instructions. Slides were gently rinsed with Hanks' BSS, fixed with methanol at 4 °C for 15 minutes, and air-dried. Chamber slides were blocked with 2% FBS-containing Hanks' BSS for 30 minutes at room temperature. HA was detected with a biotinylated HA-binding protein (Calbiochem-EMD Millipore) at 5 μg/ml and the cell membrane was stained for CD44 (clone A3D8, Sigma) were incubated overnight at 4°C in Hanks' BSS containing 2% FBS. After washing the slides three times with Hanks' BSS, secondary reagents in Hanks' BSS containing 2% FBS (AlexaFluor 488-tagged streptavidin, anti-mouse AlexaFluor 568 each at a 1:500 dilution) were incubated for 1 hour at room temperature. The slides were then washed and mounted with Vectashield mounting medium containing DAPI (Vector Laboratories). A Leica upright microscope DM5500 B (Leica), HCX PLAN APO ×20/1.32NA oil immersion objective, QImaging Retiga cooled CCD camera, and QCapture Suite software (QImaging) were used to capture all images.

Separation of Human Leukocytes

The heparinized peripheral blood (100 units heparin/ml) was subjected to Ficoll-Hypaque density gradient centrifugation to isolate total mononuclear cells. The isolated cells were resuspended in RPMI 1640 medium supplemented with 5% FBS ($25–50 \times 10^6$ cells/ml). Viability of PBMCs was confirmed to be greater than 95% by trypan blue dye exclusion.

PBMC Adhesion Assay

M-SMCs were cultured in 48-well culture dishes and allowed to grow to confluence for 2–3 days before assay and PBMC adhesion as before [17]. In brief, Poly(I·C) treatment (100 μg/ml) was applied to M-SMCs in the presence or absence of NG4 or NG5 mAbs (500 ng/mL) 18 hours prior to the adhesion phase of the assay. On the day of the adhesion assay, PBMCs (up to 70×10^6 cells/ml) were labeled with 4 μM Calcein-AM (ThermoFisher) according to manufacturer's specifications. PBMCs were washed, counted, and resuspended at 2×10^6 live cells per mL. PBMCs were added to M-SMC cultures (1×10^6 PBMC / mL) and allowed to adhere for 1hr at 4 °C. Cells were then washed 3x with ice-cold PBS, fixed with 4% PFA, and PBMC adhesion was measured by detecting Calcein AM-labeled PBMCs bound to M-SMCs using an automated Leica DM5500 B upright microscope inverted microscope in well-scan mode at 20× magnification. Image-Pro Plus acquisition software was used to enumerate PBMCs based on fluorescence and size. Streptomyces hyaluronidase treatment (1mU/mL) was performed for 30 minutes at 37 °C prior to addition of PBMCs as a control for HA dependent adhesion. (100740–1, Seikagaku, East Falmouth, MA).

Generation of HA and HC:HA Coated Culture Surfaces

The surface of CovaLink NH 96-well was used to perform covalent coupling of HA or HC-HA, following the methodology described in previous studies[50, 82]. Briefly, 8-well strips of a 96-well plate were covalently attached to HA, while HC:HA was generated in a second reaction as described below. Control wells were not coupled with HA. To each well of the 96 wells on a Nunc NH-Covalink plate (Thermo Scientific), a 46 Mm Sulfo-NHS (Thermo Scientific), 2ug of 1M Da HA (LifeCore Biomedical) in water, and 1.85 mM 1-ethyl-3-[3-dimethylaminopropyl]carbodiimide hydrochloride (EDC) (Thermo Scientific) was added to each well and the plate as sealed and incubated at room temperature for 2 hours, followed by an overnight at 4 °C. All wells were washed 2x with 2M NaCl, and 3x with PBS. To generate HC:HA, a mixture of 0.15 μg/ml recombinant human TSG6 (R&D Systems), 4 μl of human serum (Equitech Bio) and 5 μl of 10 Mm MgCl2 was incubated at 37 °C for 2 hours in a volume of 100 uL. The reaction was stopped by adding 50 μl of 20 mm EDTA to each well and washed 3x with 2M NaCl containing 50 mM MgSO4 and 3x with PBS.

Flow Cytometry Measurement of U937 Monocyte Surface Markers

U937 cells were collected after incubation with various HA matrices, resuspended in FACS buffer (PBS with 2% FBS and 1 mM EDTA), blocked with anti-human FcR antibody (Miltenyi) for 30 min at 4°C in a 96 well plate. U937 cells were then stained with antibodies against CD11b (Clone M1/70, BV421, BD Biosciences), CD38 (Clone HB7, FITC, BD Biosciences), CD163 (Clone MAC2–158, PE, BD Biosciences) or Isotype controls (BioLegend) for 45 minutes. After staining, cells were washed 3x with FACS buffer, fixed with 2% FACS-Lyse (BD Biosciences) and run on a Beckman Coulter Cytoflex located in the Utah Flow Cytometry Core within 24 h of fixation. Data were analyzed with Flow Jo (Tree Star, OR, USA). Surface expression was quantified by mean fluorescence intensity (MFI) normalized to Isotype Controls.

Immunoblot Analysis

M-SMCs and U937 cells were prepared for western blot as previously reported [17]. For colon tissue specimens, 50 mg wet tissue weight was homogenized with 5 mm diameter stainless steel beads (Qiagen, Germany) in 200 μL RIPA buffer supplemented with a protease inhibitor cocktail (Sigma) for 10 min at 4°C using a bead-homogenizer. Bead homogenates were centrifuged for 10 min at 13000 RPM at 4°C and the supernatant was collected and measured for protein content by micro-BCA assay (Thermo). Equal quantities (20μg) of protein from each sample were separated by SDS-PAGE, transferred onto polyvinylidene difluoride membranes, blocked for 1 hour with LI-COR and incubated with antibodies against TSG6 (NG4 or NG5), IαI, HC1, IRF5, or GAPDH at a 1:1000 dilution in LI-COR blocking buffer (with 0.1% Tween 20) overnight at 4°C. Membranes were washed 5x times with wash buffer (PBS containing 0.1% Tween 20), incubated with IRDye 800CW secondary antibodies (LI-COR) for 45 minutes, washed 3x as above, 1x with water, and analyzed using an Odyssey CLx infrared scanner (LI-COR). Densitometry analysis was normalized to their corresponding loading controls using ImageJ (NIH, Bethesda MD).

Serum Cytokine and HA Analysis

Mouse serum was isolated from blood using serum separator tubes (Becton Dickenson) and stored at −80°C. Serum was analyzed with a Mouse Cytokine/Chemokine Multiplex Array (MilliporeSigma catalog# MCYTMAG70PMX32BK) on a Luminex 200 instrument per manufacturer's specifications. Serum and tissue HA levels were measured in a competitive ELISA-like assay from Eschelon Biosciences. MCP1 levels secreted by U937 cells were measured using 100uL of culture medium by ELISA (Biolegend) according to manufacturer's protocol. ELISA plates were measured on a SpectraMax 340PC384 (Molecular Devices).

HA Isolation and Sizing

The lamina propria was dissected from human colon tissue specimens. HA was purified from 200mg wet weight human tissue or murine colon. Tissue was incubated with proteinase-K at a concentration of 0.5 mg/mL in phosphate-buffered saline for 18 hours at 60°C, followed by treatment with endonuclease from Serratia marcescens (Benzonase) at a concentration of 50 U/mL for 1 hour at 37°C. Samples were dialyzed against 0.1 mol/L NaCl, run over anion exchange spin columns (Thermo Fisher Scientific), washed with increasing concentrations of NaCl (0.1M, 0.2M, 0.25M, 0.3M) and followed by an 0.8M NaCl to elute bound HA. Samples were dialyzed with water for 24 hours, concentrated, and analyzed using 0.5% agarose sizing gels at stained with Stains-All as previously described[83]. Treatment of samples with Streptomyces hyaluronidase (2 U/mL for one hour at 37°C) is used as a specificity control to confirm the identity of HA in the gel. Low-molecular weight HA was estimated by fractionating an aliquot of purified HA over a 100 kDa molecular-weight cut off membrane and measuring total HA to the <100k Da eluate by competitive HA (Echelon Biosciences).

Quantitative Real-Time PCR

RNA was isolated from human tissues, murine tissues, M-SMCs, and U937 cells with a RNAeasy kit (Qiagen) according to manufacturer's specifications. Eluted RNA (30uL volume in water) was treated with DNase to remove genomic DNA. Reverse transcription was performed using M-MLV Reverse Transcriptase (Thermo Fisher Scientific) and oligo-d(T) primers, as per the manufacturer's instructions. cDNA products were stored at −20°C until analyzed by real-time quantitative PCR. Validated primers for TSG6, HAS1, HAS2, HAS3, MCP1, and 18S rRNA, which included 6-carboxyfluorescein (FAM) probes, were obtained from Applied Biosystems (Invitrogen, Carlsbad, CA). Real-time PCR amplification was performed using TaqMan gene expression Master Mix, primers and fluorogenic probes (Invitrogen), and cDNA in 25-μL reaction volumes. The reactions were carried out in quadruplicate using a Bio-Rad C1000 Touch Thermal Cycler with attached CFX96 Real-Time System (Bio-Rad Laboratories) using manufacturer's recommended PCR conditions. All data were analyzed using Bio-Rad CFX Manager software version 2.1 (Bio-Rad Laboratories), and the Livak (ΔΔCT) method was used to calculate changes in gene expression.

TSG6 HC-Transferase Assay

Assay of TSG6 HC-Transferase assay was performed as previously described with minor modifications [43]. Human serum purchased from Equitech-Bio Inc was used as the source of IαI and pre-IαI as HC donors. Recombinant human TSG6 was obtained from R&D Systems, HA-14 from Hyalose, and anti-IαI from Dako (clone: A0301) were used. All experiments used human serum dialyzed into PBS containing 1 mM MgCl2. The reaction volumes were 25 μL of PBS containing 1 mM MgCl2, 5% serum supplemented with 1.25 μg HA, 5 ng of TSG-6. All monoclonal antibodies (NG4, NG5) were added at an equimolar ratio (1:1) with TSG6. TSG6 was always added last and was used to denote the start time of the assay. Reactions were stopped by addition of EDTA (80mM final concentration) to assay tubes. All anti-TSG6 monoclonal antibodies were provided by Dr. Tibor Glant.

Supplementary Material

Refer to Web version on PubMed Central for supplementary material.

ACKNOWLEDGEMENTS

The authors thank Gail West for assistance with cell isolation, Carol de la Motte and Claudio Fiocchi for helpful conversations, Satya Kurada for assistance with IBD patient samples, Rebecca Mellema for careful reading of the manuscript. We also acknowledge Vincent Hascall for providing the TSG6 KO mice and Tibor Glant for TSG6 antibodies. Finally, the authors thank our departed friend and colleague Mark E. Lauer for his helpful discussions, guidance, and mentorship.

SOURCES OF FUNDING

This work was financially supported by the National Institutes of Health (R00HL135265, R01HL167919) (A.C.P.) and in part by the Programs of Excellence in Glycosciences (HL107147) from the National Heart, Lung, and Blood Institute.

Non-standard abbreviations and acronyms

ECM	Extracellular Matrix
HA	hyaluronan or hyaluronic acid
HAS	Hyaluronan Synthase
HC	heavy chain protein component from inter-α-inhibitor
HC:HA	a complex of HC protein from IαI covalently linked to HA
IαI	inter-α-inhibitor
IRF5	interferon-regulatory factor 5
DSS	dextran sulfate sodium
TSG6	Tumor necrosis factor-alpha stimulated gene-6
4MU	4-methylumbilifferone

REFERENCES

[1]. Gerdin B, Hallgren R, Localisation of hyaluronan in the human intestinal wall, Gut 32(7) (1991) 760–2. [PubMed: 1713183]

[2]. Weigel PH, Hascall VC, Tammi M, Hyaluronan synthases J Biol Chem 272(22) (1997) 13997–4000.

[3]. Day AJ, Milner CM, TSG-6: A multifunctional protein with anti-inflammatory and tissue-protective properties, Matrix Biol 78–79 (2019) 60–83.

[4]. Milner CM, Day AJ, TSG-6: a multifunctional protein associated with inflammation, J Cell Sci 116(Pt 10) (2003) 1863–73. [PubMed: 12692188]

[5]. Sivakumar A, Mahadevan A, Lauer ME, Narvaez RJ, Ramesh S, Demler CM, Souchet NR, Hascall VC, Midura RJ, Garantziotis S, Frank DB, Kimata K, Kurpios NA, Midgut Laterality Is Driven by Hyaluronan on the Right, Dev Cell 46(5) (2018) 533–551 e5. [PubMed: 30174180]

[6]. Hamm A, Veeck J, Bektas N, Wild PJ, Hartmann A, Heindrichs U, Kristiansen G, Werbowetski-Ogilvie T, Del Maestro R, Knuechel R, Dahl E, Frequent expression loss of Inter-alpha-trypsin inhibitor heavy chain (ITIH) genes in multiple human solid tumors: a systematic expression analysis, BMC Cancer 8 (2008) 25. [PubMed: 18226209]

[7]. Yingsung W, Zhuo L, Morgelin M, Yoneda M, Kida D, Watanabe H, Ishiguro N, Iwata H, Kimata K, Molecular heterogeneity of the SHAP-hyaluronan complex. Isolation and characterization of the complex in synovial fluid from patients with rheumatoid arthritis, The Journal of biological chemistry 278(35) (2003) 32710–8. [PubMed: 12799384]

[8]. Zhuo L, Kanamori A, Kannagi R, Itano N, Wu J, Hamaguchi M, Ishiguro N, Kimata K, SHAP potentiates the CD44-mediated leukocyte adhesion to the hyaluronan substratum, J Biol Chem 281(29) (2006) 20303–14. [PubMed: 16702221]

[9]. Lauer ME, Majors AK, Comhair S, Ruple LM, Matuska B, Subramanian A, Farver C, Dworski R, Grandon D, Laskowski D, Dweik RA, Erzurum SC, Hascall VC, Aronica MA, Hyaluronan and Its Heavy Chain Modification in Asthma Severity and Experimental Asthma Exacerbation, Biol Chem 290(38) (2015) 23124–34.

[10]. Swaidani S, Cheng G, Lauer ME, Sharma M, Mikecz K, Hascall VC, Aronica MA, TSG-6 protein is crucial for the development of pulmonary hyaluronan deposition, eosinophilia, and airway hyperresponsiveness in a murine model of asthma, J Biol Chem 288(1) (2013) 412–22. [PubMed: 23118230]

[11]. Zhang S, He H, Day AJ, Tseng SC, Constitutive expression of inter-alpha-inhibitor (IalphaI) family proteins and tumor necrosis factor-stimulated gene-6 (TSG-6) by human amniotic membrane epithelial and stromal cells supporting formation of the heavy chain-hyaluronan (HC-HA) complex, J Biol Chem 287(15) (2012) 12433–44. [PubMed: 22351758]

[12]. Zhuo L, Hascall VC, Kimata K, Inter-alpha-trypsin inhibitor, a covalent protein-glycosaminoglycan-protein complex, The Journal of biological chemistry 279(37) (2004) 38079–82. [PubMed: 15151994]

[13]. Day AJ, de la Motte CA, Hyaluronan cross-linking: a protective mechanism in inflammation?, Trends in immunology 26(12) (2005) 637–43. [PubMed: 16214414]

[14]. de La Motte CA, Hascall VC, Calabro A, Yen-Lieberman B, Strong SA, Mononuclear leukocytes preferentially bind via CD44 to hyaluronan on human intestinal mucosal smooth muscle cells after virus infection or treatment with poly(I.C), J Biol Chem 274(43) (1999) 30747–55. [PubMed: 10521464]

[15]. de la Motte CA, Hascall VC, Drazba J, Bandyopadhyay SK, Strong SA, Mononuclear leukocytes bind to specific hyaluronan structures on colon mucosal smooth muscle cells treated with polyinosinic acid:polycytidylic acid: inter-alpha-trypsin inhibitor is crucial to structure and function, Am J Pathol 163(1) (2003) 121–33. [PubMed: 12819017]

[16]. Kessler S, Rho H, West G, Fiocchi C, Drazba J, de la Motte C, Hyaluronan (HA) deposition precedes and promotes leukocyte recruitment in intestinal inflammation, Clin Transl Sci 1(1) (2008) 57–61. [PubMed: 20443819]

[17]. Petrey AC, de la Motte CA, Thrombin Cleavage of Inter-alpha-inhibitor Heavy Chain 1 Regulates Leukocyte Binding to an Inflammatory Hyaluronan Matrix, J Biol Chem 291(47) (2016) 24324–24334. [PubMed: 27679489]

[18]. Petrey AC, Obery DR, Kessler SP, Zawerton A, Flamion B, de la Motte CA, Platelet hyaluronidase-2 regulates the early stages of inflammatory disease in colitis, Blood 134(9) (2019) 765–775. [PubMed: 31262781]

[19]. Fiocchi C, Intestinal inflammation: a complex interplay of immune and nonimmune cell interactions, The American journal of physiology 273(4 Pt 1) (1997) G769–75. [PubMed: 9357817]

[20]. Ouyang Q, Tandon R, Goh KL, Ooi CJ, Ogata H, Fiocchi C, The emergence of inflammatory bowel disease in the Asian Pacific region, Curr Opin Gastroenterol 21(4) (2005) 408–13. [PubMed: 15930979]

[21]. Vermeire S, Towards a novel molecular classification of IBD, Dig Dis 30(4) (2012) 425–7. [PubMed: 22796810]

[22]. Vermeire S, Van Assche G, Rutgeerts P, Classification of inflammatory bowel disease: the old and the new, Curr Opin Gastroenterol 28(4) (2012) 321–6. [PubMed: 22647554]

[23]. Ananthakrishnan AN, Epidemiology and risk factors for IBD, Nat Rev Gastroenterol Hepatol 12(4) (2015) 205–17. [PubMed: 25732745]

[24]. Jostins L, Ripke S, Weersma RK, Duerr RH, McGovern DP, Hui KY, Lee JC, Schumm LP, Sharma Y, Anderson CA, Essers J, Mitrovic M, Ning K, Cleynen I, Theatre E, Spain SL, Raychaudhuri S, Goyette P, Wei Z, Abraham C, Achkar JP, Ahmad T, Amininejad L, Ananthakrishnan AN, Andersen V, Andrews JM, Baidoo L, Balschun T, Bampton PA, Bitton A, Boucher G, Brand S, Buning C, Cohain A, Cichon S, D'Amato M, De Jong D, Devaney KL, Dubinsky M, Edwards C, Ellinghaus D, Ferguson LR, Franchimont D, Fransen K, Gearry R, Georges M, Gieger C, Glas J, Haritunians T, Hart A, Hawkey C, Hedl M, Hu X, Karlsen TH, Kupcinskas L, Kugathasan S, Latiano A, Laukens D, Lawrance IC, Lees CW, Louis E, Mahy G, Mansfield J, Morgan AR, Mowat C, Newman W, Palmieri O, Ponsioen CY, Potocnik U, Prescott NJ, Regueiro M, Rotter JI, Russell RK, Sanderson JD, Sans M, Satsangi J, Schreiber S, Simms LA, Sventoraityte J, Targan SR, Taylor KD, Tremelling M, Verspaget HW, De Vos M, Wijmenga C, Wilson DC, Winkelmann J, Xavier RJ, Zeissig S, Zhang B, Zhang CK, Zhao H, International IBDGC, Silverberg MS, Annese V, Hakonarson H, Brant SR, Radford-Smith G, Mathew CG, Rioux JD, Schadt EE, Daly MJ, Franke A, Parkes M, Vermeire S, Barrett JC, Cho JH, Host-microbe interactions have shaped the genetic architecture of inflammatory bowel disease, Nature 491(7422) (2012) 119–24. [PubMed: 23128233]

[25]. de Souza HS, Fiocchi C, Immunopathogenesis of IBD: current state of the art, Nat Rev Gastroenterol Hepatol 13(1) (2016) 13–27. [PubMed: 26627550]

[26]. Shimshoni E, Yablecovitch D, Baram L, Dotan I, Sagi I, ECM remodelling in IBD: innocent bystander or partner in crime? The emerging role of extracellular molecular events in sustaining intestinal inflammation, Gut 64(3) (2015) 367–72. [PubMed: 25416065]

[27]. Mukhopadhyay D, Asari A, Rugg MS, Day AJ, Fulop C, Specificity of the tumor necrosis factor-induced protein 6-mediated heavy chain transfer from inter-alpha-trypsin inhibitor to hyaluronan: implications for the assembly of the cumulus extracellular matrix, The Journal of biological chemistry 279(12) (2004) 11119–28. [PubMed: 14707130]

[28]. Rugg MS, Willis AC, Mukhopadhyay D, Hascall VC, Fries E, Fulop C, Milner CM, Day AJ, Characterization of complexes formed between TSG-6 and inter-alpha-inhibitor that act as intermediates in the covalent transfer of heavy chains onto hyaluronan, The Journal of biological chemistry 280(27) (2005) 25674–86. [PubMed: 15840581]

[29]. Termeer C, Benedix F, Sleeman J, Fieber C, Voith U, Ahrens T, Miyake K, Freudenberg M, Galanos C, Simon JC, Oligosaccharides of Hyaluronan activate dendritic cells via toll-like receptor 4, J Exp Med 195(1) (2002) 99–111. [PubMed: 11781369]

[30]. Hundhausen C, Schneckmann R, Ostendorf Y, Rimpler J, von Glinski A, Kohlmorgen C, Pasch N, Rolauer L, von Ameln F, Eckermann O, Altschmied J, Ale-Agha N, Haendeler J, Flogel U, Fischer JW, Grandoch M, Endothelial hyaluronan synthase 3 aggravates acute colitis in an experimental model of inflammatory bowel disease, Matrix Biol 102 (2021) 20–36. [PubMed: 34464693]

[31]. Yamaguchi Y, Noda H, Okaniwa N, Adachi K, Shinmura T, Nakagawa S, Ebi M, Ogasawara N, Funaki Y, Zhuo L, Kimata K, Sasaki M, Kasugai K, Serum-Derived Hyaluronan-Associated Protein Is a Novel Biomarker for Inflammatory Bowel Diseases, Digestion 95(2) (2017) 146–155. [PubMed: 28161704]

[32]. de la Motte C, Nigro J, Vasanji A, Rho H, Kessler S, Bandyopadhyay S, Danese S, Fiocchi C, Stern R, Platelet-derived hyaluronidase 2 cleaves hyaluronan into fragments that trigger monocyte-mediated production of proinflammatory cytokines, Am J Pathol 174(6) (2009) 2254–64. [PubMed: 19443707]

[33]. Perse M, Cerar A, Dextran sodium sulphate colitis mouse model: traps and tricks, J Biomed Biotechnol 2012 (2012) 718617. [PubMed: 22665990]

[34]. Meshkibaf S, Martins AJ, Henry GT, Kim SO, Protective role of G-CSF in dextran sulfate sodium-induced acute colitis through generating gut-homing macrophages, Cytokine 78 (2016) 69–78. [PubMed: 26687628]

[35]. Li B, Alli R, Vogel P, Geiger TL, IL-10 modulates DSS-induced colitis through a macrophage-ROS-NO axis, Mucosal Immunol 7(4) (2014) 869–78. [PubMed: 24301657]

[36]. Beck-Schimmer B, Oertli B, Pasch T, Wuthrich RP, Hyaluronan induces monocyte chemoattractant protein-1 expression in renal tubular epithelial cells, J Am Soc Nephrol 9(12) (1998) 2283–90. [PubMed: 9848782]

[37]. Hodge-Dufour J, Noble PW, Horton MR, Bao C, Wysoka M, Burdick MD, Strieter RM, Trinchieri G, Pure E, Induction of IL-12 and chemokines by hyaluronan requires adhesion-dependent priming of resident but not elicited macrophages, J Immunol 159(5) (1997) 2492–500. [PubMed: 9278343]

[38]. Webber J, Meran S, Steadman R, Phillips A, Hyaluronan orchestrates transforming growth factor-beta1-dependent maintenance of myofibroblast phenotype, J Biol Chem 284(14) (2009) 9083–92. [PubMed: 19193641]

[39]. Mukhopadhyay D, Hascall VC, Day AJ, Salustri A, Fulop C, Two distinct populations of tumor necrosis factor-stimulated gene-6 protein in the extracellular matrix of expanded mouse cumulus cell-oocyte complexes, Arch Biochem Biophys 394(2) (2001) 173–81. [PubMed: 11594731]

[40]. Briggs DC, Birchenough HL, Ali T, Rugg MS, Waltho JP, Ievoli E, Jowitt TA, Enghild JJ, Richter RP, Salustri A, Milner CM, Day AJ, Metal Ion-dependent Heavy Chain Transfer Activity of TSG-6 Mediates Assembly of the Cumulus-Oocyte Matrix, J Biol Chem 290(48) (2015) 28708–23. [PubMed: 26468290]

[41]. Salustri A, Garlanda C, Hirsch E, De Acetis M, Maccagno A, Bottazzi B, Doni A, Bastone A, Mantovani G, Beck Peccoz P, Salvatori G, Mahoney DJ, Day AJ, Siracusa G, Romani L, Mantovani A, PTX3 plays a key role in the organization of the cumulus oophorus extracellular matrix and in in vivo fertilization, Development 131(7) (2004) 1577–86. [PubMed: 14998931]

[42]. Nagyeri G, Radacs M, Ghassemi-Nejad S, Tryniszewska B, Olasz K, Hutas G, Gyorfy Z, Hascall VC, Glant TT, Mikecz K, TSG-6 protein, a negative regulator of inflammatory arthritis, forms a ternary complex with murine mast cell tryptases and heparin, J Biol Chem 286(26) (2011) 23559–69. [PubMed: 21566135]

[43]. Lauer ME, Glant TT, Mikecz K, DeAngelis PL, Haller FM, Husni ME, Hascall VC, Calabro A, Irreversible heavy chain transfer to hyaluronan oligosaccharides by tumor necrosis factor-stimulated gene-6, J Biol Chem 288(1) (2013) 205–14. [PubMed: 23166324]

[44]. He H, Zhang S, Tighe S, Son J, Tseng SCG, Immobilized heavy chain-hyaluronic acid polarizes lipopolysaccharide-activated macrophages toward M2 phenotype, J Biol Chem 288(36) (2013) 25792–25803. [PubMed: 23878196]

[45]. Sala E, Genua M, Petti L, Anselmo A, Arena V, Cibella J, Zanotti L, D'Alessio S, Scaldaferri F, Luca G, Arato I, Calafiore R, Sgambato A, Rutella S, Locati M, Danese S, Vetrano S, Mesenchymal Stem Cells Reduce Colitis in Mice via Release of TSG6, Independently of Their Localization to the Intestine, Gastroenterology 149(1) (2015) 163–176 e20. [PubMed: 25790743]

[46]. Song WJ, Li Q, Ryu MO, Ahn JO, Bhang DH, Jung YC, Youn HY, TSG-6 released from intraperitoneally injected canine adipose tissue-derived mesenchymal stem cells ameliorate inflammatory bowel disease by inducing M2 macrophage switch in mice, Stem Cell Res Ther 9(1) (2018) 91. [PubMed: 29625582]

[47]. Song WJ, Li Q, Ryu MO, Ahn JO, Ha Bhang D, Chan Jung Y, Youn HY, TSG-6 Secreted by Human Adipose Tissue-derived Mesenchymal Stem Cells Ameliorates DSS-induced colitis by Inducing M2 Macrophage Polarization in Mice, Sci Rep 7(1) (2017) 5187. [PubMed: 28701721]

[48]. Zhang S, Fang J, Liu Z, Hou P, Cao L, Zhang Y, Liu R, Li Y, Shang Q, Chen Y, Feng C, Wang G, Melino G, Wang Y, Shao C, Shi Y, Inflammatory cytokines-stimulated human muscle stem cells ameliorate ulcerative colitis via the IDO-TSG6 axis, Stem Cell Res Ther 12(1) (2021) 50. [PubMed: 33422134]

[49]. Mittal M, Tiruppathi C, Nepal S, Zhao YY, Grzych D, Soni D, Prockop DJ, Malik AB, TNFalpha-stimulated gene-6 (TSG6) activates macrophage phenotype transition to prevent inflammatory lung injury, Proc Natl Acad Sci U S A 113(50) (2016) E8151–E8158. [PubMed: 27911817]

[50]. He H, Li W, Tseng DY, Zhang S, Chen SY, Day AJ, Tseng SC, Biochemical characterization and function of complexes formed by hyaluronan and the heavy chains of inter-alpha-inhibitor (HC*HA) purified from extracts of human amniotic membrane, J Biol Chem 284(30) (2009) 20136–46. [PubMed: 19491101]

[51]. Krausgruber T, Blazek K, Smallie T, Alzabin S, Lockstone H, Sahgal N, Hussell T, Feldmann M, Udalova IA, IRF5 promotes inflammatory macrophage polarization and TH1-TH17 responses, Nat Immunol 12(3) (2011) 231–8. [PubMed: 21240265]

[52]. Paun A, Reinert JT, Jiang Z, Medin C, Balkhi MY, Fitzgerald KA, Pitha PM, Functional characterization of murine interferon regulatory factor 5 (IRF-5) and its role in the innate antiviral response, J Biol Chem 283(21) (2008) 14295–308. [PubMed: 18332133]

[53]. Corbin AL, Gomez-Vazquez M, Berthold DL, Attar M, Arnold IC, Powrie FM, Sansom SN, Udalova IA, IRF5 guides monocytes toward an inflammatory CD11c(+) macrophage phenotype and promotes intestinal inflammation, Sci Immunol 5(47) (2020).

[54]. Lee TH, Lee GW, Ziff EB, Vilcek J, Isolation and characterization of eight tumor necrosis factor-induced gene sequences from human fibroblasts, Mol Cell Biol 10(5) (1990) 1982–8. [PubMed: 2183014]

[55]. Lee TH, Wisniewski HG, Vilcek J, A novel secretory tumor necrosis factor-inducible protein (TSG-6) is a member of the family of hyaluronate binding proteins, closely related to the adhesion receptor CD44, J Cell Biol 116(2) (1992) 545–57. [PubMed: 1730767]

[56]. Szanto S, Bardos T, Gal I, Glant TT, Mikecz K, Enhanced neutrophil extravasation and rapid progression of proteoglycan-induced arthritis in TSG-6-knockout mice, Arthritis Rheum 50(9) (2004) 3012–22. [PubMed: 15457471]

[57]. Mindrescu C, Dias AA, Olszewski RJ, Klein MJ, Reis LF, Wisniewski HG, Reduced susceptibility to collagen-induced arthritis in DBA/1J mice expressing the TSG-6 transgene, Arthritis Rheum 46(9) (2002) 2453–64. [PubMed: 12355494]

[58]. Sammarco G, Shalaby M, Elangovan S, Petti L, Roda G, Restelli S, Arena V, Ungaro F, Fiorino G, Day AJ, D'Alessio S, Vetrano S, Hyaluronan Accelerates Intestinal Mucosal Healing through Interaction with TSG-6, Cells 8(9) (2019).

[59]. Zhang C, Zhang B, Wang H, Tao Q, Ge S, Zhai Z, Tumor necrosis factor alpha-stimulated gene-6 (TSG-6) inhibits the inflammatory response by inhibiting the activation of P38 and JNK signaling pathway and decreases the restenosis of vein grafts in rats, Heart Vessels 32(12) (2017) 1536–1545. [PubMed: 28975447]

[60]. Tuo J, Cao X, Shen D, Wang Y, Zhang J, Oh JY, Prockop DJ, Chan CC, Anti-inflammatory recombinant TSG-6 stabilizes the progression of focal retinal degeneration in a murine model, J Neuroinflammation 9 (2012) 59. [PubMed: 22452753]

[61]. Mindrescu C, Thorbecke GJ, Klein MJ, Vilcek J, Wisniewski HG, Amelioration of collagen-induced arthritis in DBA/1J mice by recombinant TSG-6, a tumor necrosis factor/interleukin-1-inducible protein, Arthritis Rheum 43(12) (2000) 2668–77. [PubMed: 11145024]

[62]. Abbadi A, Lauer M, Swaidani S, Wang A, Hascall V, Hyaluronan Rafts on Airway Epithelial Cells, J Biol Chem 291(3) (2016) 1448–55. [PubMed: 26601955]

[63]. Janssen U, Thomas G, Glant T, Phillips A, Expression of inter-alpha-trypsin inhibitor and tumor necrosis factor-stimulated gene 6 in renal proximal tubular epithelial cells, Kidney Int 60(1) (2001) 126–36. [PubMed: 11422744]

[64]. Kim Y, Kessler SP, Obery DR, Homer CR, McDonald C, de la Motte CA, Hyaluronan 35kDa treatment protects mice from Citrobacter rodentium infection and induces epithelial tight junction protein ZO-1 in vivo, Matrix Biol 62 (2017) 28–39. [PubMed: 27845198]

[65]. Hill DR, Kessler SP, Rho HK, Cowman MK, de la Motte CA, Specific-sized hyaluronan fragments promote expression of human beta-defensin 2 in intestinal epithelium, J Biol Chem 287(36) (2012) 30610–24. [PubMed: 22761444]

[66]. Kessler SP, Obery DR, Nickerson KP, Petrey AC, McDonald C, de la Motte CA, Multifunctional Role of 35 Kilodalton Hyaluronan in Promoting Defense of the Intestinal Epithelium, J Histochem Cytochem 66(4) (2018) 273–287. [PubMed: 29290146]

[67]. Hill DR, Rho HK, Kessler SP, Amin R, Homer CR, McDonald C, Cowman MK, de la Motte CA, Human milk hyaluronan enhances innate defense of the intestinal epithelium, J Biol Chem 288(40) (2013) 29090–104. [PubMed: 23950179]

[68]. Kim Y, West GA, Ray G, Kessler SP, Petrey AC, Fiocchi C, McDonald C, Longworth MS, Nagy LE, de la Motte CA, Layilin is critical for mediating hyaluronan 35kDa-induced intestinal epithelial tight junction protein ZO-1 in vitro and in vivo, Matrix Biol 66 (2018) 93–109. [PubMed: 28978412]

[69]. Petrey AC, de la Motte CA, Hyaluronan in inflammatory bowel disease: Cross-linking inflammation and coagulation, Matrix Biol 78–79 (2019) 314–323.

[70]. Wei HX, Wang B, Li B, IL-10 and IL-22 in Mucosal Immunity: Driving Protection and Pathology, Front Immunol 11 (2020) 1315. [PubMed: 32670290]

[71]. Koelink PJ, Bloemendaal FM, Li B, Westera L, Vogels EWM, van Roest M, Gloudemans AK, van ‘t Wout AB, Korf H, Vermeire S, Te Velde AA, Ponsioen CY, D’Haens GR, Verbeek JS, Geiger TL, Wildenberg ME, van den Brink GR, Anti-TNF therapy in IBD exerts its therapeutic effect through macrophage IL-10 signalling, Gut 69(6) (2020) 1053–1063. [PubMed: 31506328]

[72]. Dharmasiri S, Garrido-Martin EM, Harris RJ, Bateman AC, Collins JE, Cummings JRF, Sanchez-Elsner T, Human Intestinal Macrophages Are Involved in the Pathology of Both Ulcerative Colitis and Crohn Disease, Inflamm Bowel Dis 27(10) (2021) 1641–1652. [PubMed: 33570153]

[73]. Soroosh A, Albeiroti S, West GA, Willard B, Fiocchi C, de la Motte CA, Crohn’s Disease Fibroblasts Overproduce the Novel Protein KIAA1199 to Create Proinflammatory Hyaluronan Fragments, Cell Mol Gastroenterol Hepatol 2(3) (2016) 358–368 e4. [PubMed: 27981209]

[74]. Kim Y, de la Motte CA, The Role of Hyaluronan Treatment in Intestinal Innate Host Defense, Front Immunol 11 (2020) 569. [PubMed: 32411124]

[75]. Zheng L, Riehl TE, Stenson WF, Regulation of colonic epithelial repair in mice by Toll-like receptors and hyaluronic acid, Gastroenterology 137(6) (2009) 2041–51. [PubMed: 19732774]

[76]. Kessler SP, Obery DR, de la Motte C, Hyaluronan Synthase 3 Null Mice Exhibit Decreased Intestinal Inflammation and Tissue Damage in the DSS-Induced Colitis Model, Int J Cell Biol 2015 (2015) 745237. [PubMed: 26448758]

[77]. Kuipers HF, Rieck M, Gurevich I, Nagy N, Butte MJ, Negrin RS, Wight TN, Steinman L, Bollyky PL, Hyaluronan synthesis is necessary for autoreactive T-cell trafficking, activation, and Th1 polarization, Proc Natl Acad Sci U S A 113(5) (2016) 1339–44. [PubMed: 26787861]

[78]. Homann S, Grandoch M, Kiene LS, Podsvyadek Y, Feldmann K, Rabausch B, Nagy N, Lehr S, Kretschmer I, Oberhuber A, Bollyky P, Fischer JW, Hyaluronan synthase 3 promotes plaque inflammation and atheroprogression, Matrix Biol 66 (2018) 67–80. [PubMed: 28987865]

[79]. Dyer DP, Thomson JM, Hermant A, Jowitt TA, Handel TM, Proudfoot AE, Day AJ, Milner CM, TSG-6 inhibits neutrophil migration via direct interaction with the chemokine CXCL8, J Immunol 192(5) (2014) 2177–85. [PubMed: 24501198]

[80]. Kieu TQ, Tazawa K, Kawashima N, Noda S, Fujii M, Nara K, Hashimoto K, Han P, Okiji T, Kinetics of LYVE-1-positive M2-like macrophages in developing and repairing dental pulp in vivo and their pro-angiogenic activity in vitro, Sci Rep 12(1) (2022) 5176. [PubMed: 35338195]

[81]. Mahler M, Bristol IJ, Leiter EH, Workman AE, Birkenmeier EH, Elson CO, Sundberg JP, Differential susceptibility of inbred mouse strains to dextran sulfate sodium-induced colitis, Am J Physiol 274(3) (1998) G544–51. [PubMed: 9530156]

[82]. Colon E, Shytuhina A, Cowman MK, Band PA, Sanggaard KW, Enghild JJ, Wisniewski HG, Transfer of inter-alpha-inhibitor heavy chains to hyaluronan by surface-linked hyaluronan-TSG-6 complexes, J Biol Chem 284(4) (2009) 2320–31. [PubMed: 19033448]

[83]. Petrey AC, Obery DR, Kessler SP, Flamion B, de la Motte CA, Hyaluronan Depolymerization by Megakaryocyte Hyaluronidase-2 Is Required for Thrombopoiesis, Am J Pathol 186(9) (2016) 2390–403. [PubMed: 27398974]

Highlights

- Patients with active IBD have increased TSG6 expression localized throughout colon layers along with submucosal deposition of HC1 and HC3
- TSG6-null mice have an aggravated inflammatory response to DSS-induced colitis characterized by a robust increase in inflammatory cytokines and chemokines
- Inhibition of TSG6 HC-transferase activity with monoclonal antibodies disrupts the HApericellular matrix and impairs formation of a leukocyte-adhesive HC:HA cables
- HC:HA interaction with activated monocytes leads to a suppressed inflammatoryresponse

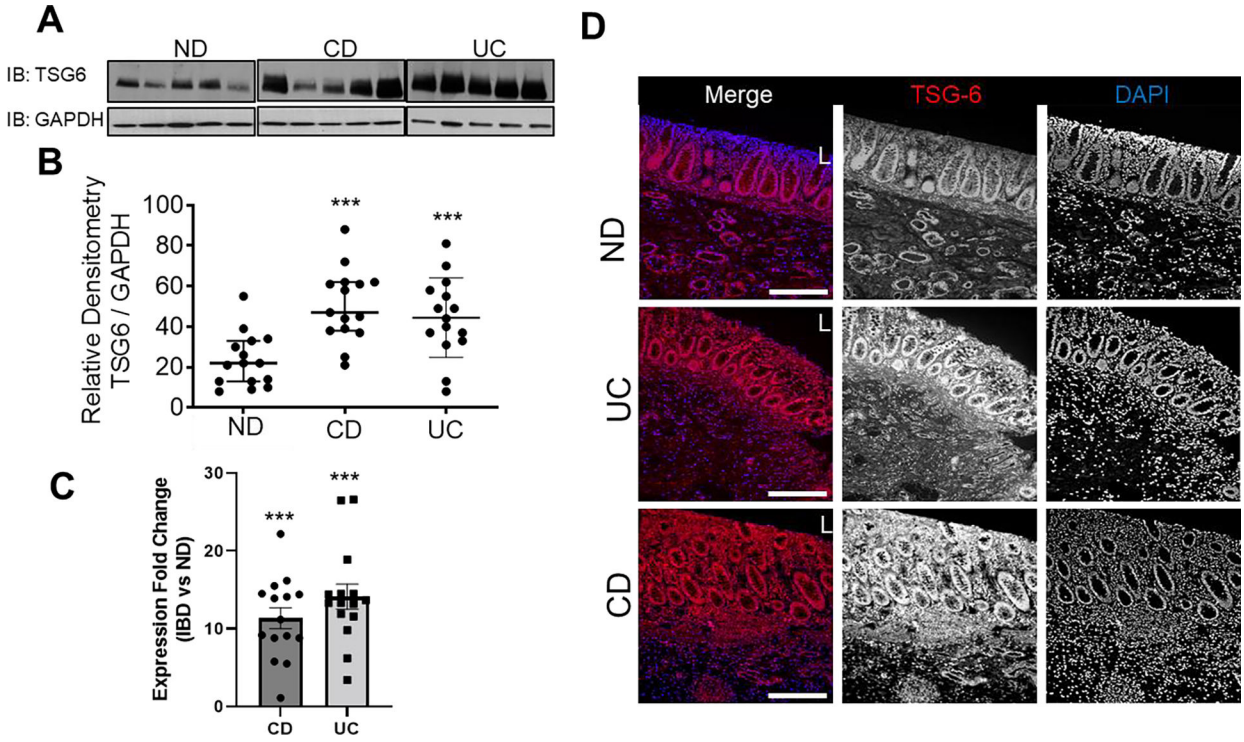

Figure 1. TSG6 is increased in colon tissue from patients with IBD.

(A) Colon tissue from non-IBD (ND), or IBD patients with active colonic disease were homogenized and TSG6 was detected by western blotting with TSG6 mAb antibody NG4. GAPDH was used as a loading control. (B) Densitometry quantification of TSG6 levels in tissue. (C) TSG6 mRNA expression normalized to r18S. (D) Confocal image of a human colon tissue sections immunostained for TSG6 protein (red) and dapi (blue). Images shown are representative of other replicates from different patients. A Leica TCS SP5 II Confocal/ Multi-Photon high-speed upright microscope with Acousto-Optical Beam Splitter was used to capture all images at 20× magnification. Leica LAS confocal software was utilized to acquire the images. Scale bars: 100 μm. Data are reported as mean ± SEM; using unpaired Student's t test, 2 tailed, with at least 3 independent experiments. Non-IBD (ND, n= 15), Crohn's disease (CD) n= 15), Ulcerative Colitis (UC) n= 15.

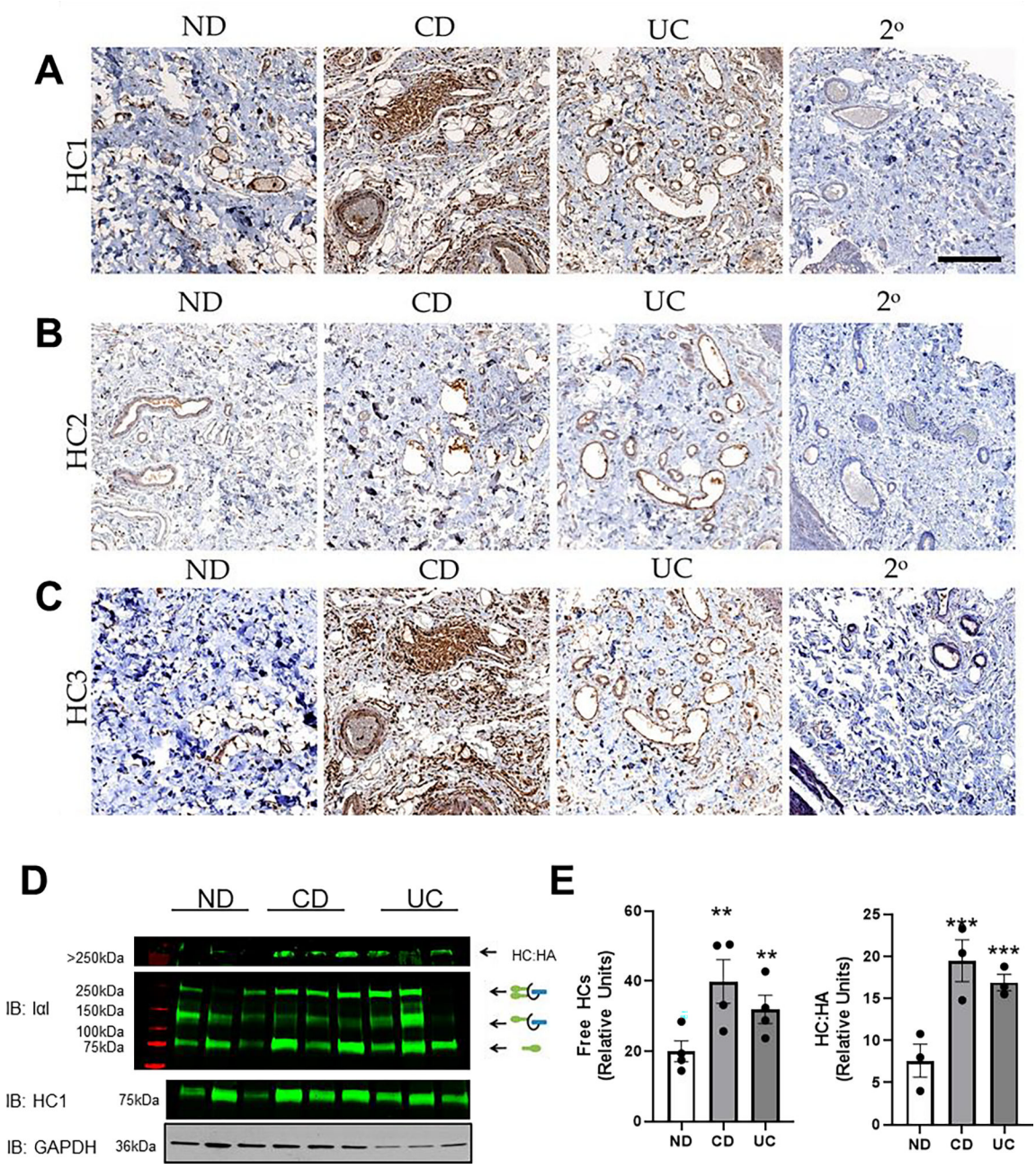

Figure 2. Accumulation of HCs in IBD Colon Tissue.

Staining for individual HCs (A-C) was performed on serial sections of paraffin embedded colon tissue from non-IBD (ND), or IBD patients with active colonic disease. A negative control (2°) section probed with all reagents except the primary HC-specific antibodies. Images shown are representative of other replicates from different patients. Images were captured at 20× magnification using a Leica Slide Scanner SCN400 (Leica) (D) 200mg of colon tissue from non-IBD (ND), or IBD patients with active colonic disease were homogenized and analyzed by western blot using antibodies that detect the HCs of IαI (cartoon shown to the right for reference), HC1, or GAPDH. (E) Densitometry quantification of free HC or HC:HA levels in tissue normalized to GAPDH. Statistical differences between

groups were determined using 1-way ANOVA with Dunn's correction. Non-IBD (ND, n= 15), Crohn's disease (CD) n= 15), Ulcerative Colitis (UC) n= 15. Data are reported as means ± SEM. $^{**}P < .01$, $^{***}P < .001$. Scale bar = 150um

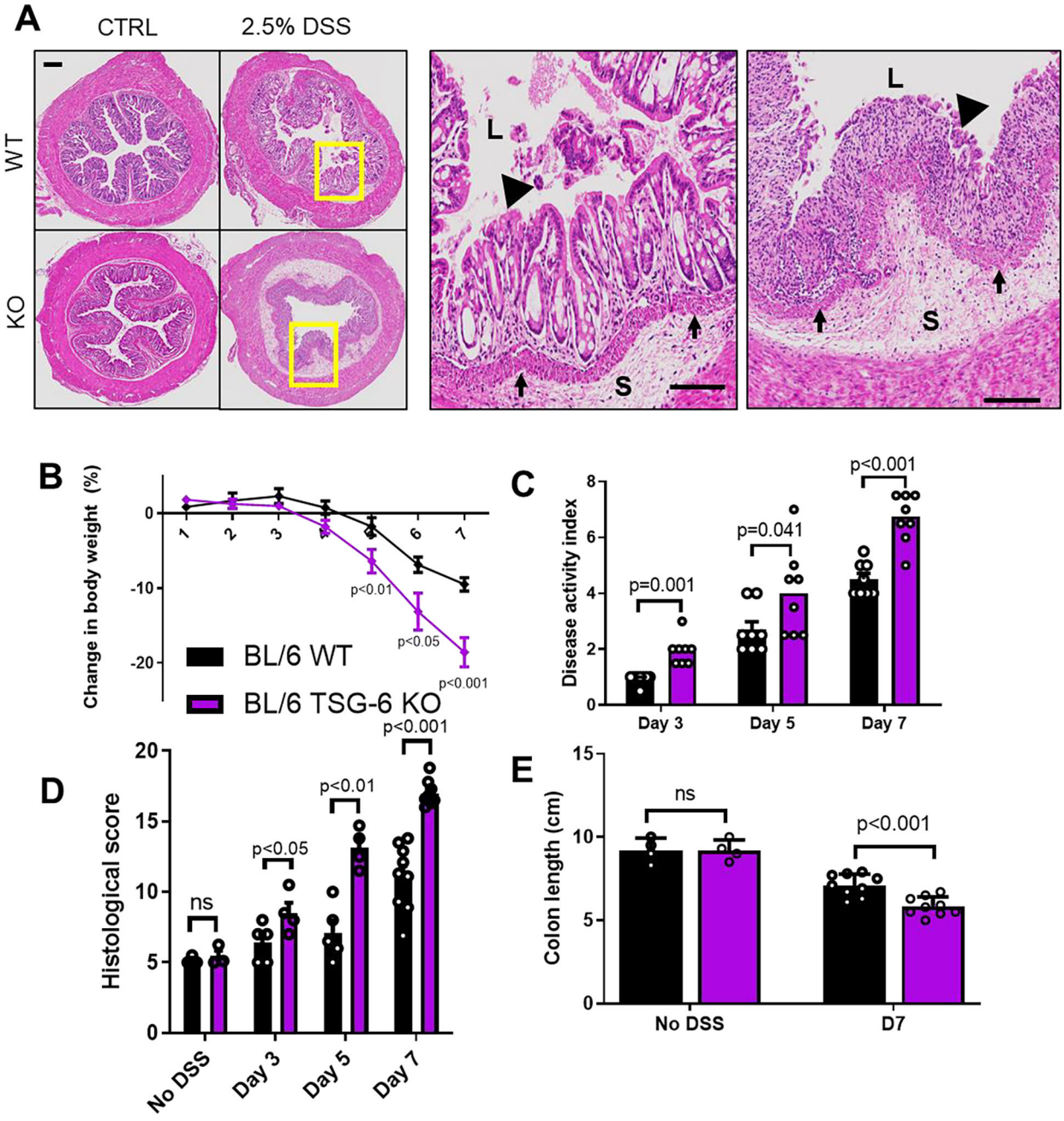

Figure 3. TSG6-deficient mice are susceptible to DSS-induced colitis.

(A) Cross-sectional images of the rectal colon were obtained on day 7 of DSS-induced colitis. H&E staining was utilized to highlight structural and cellular modifications in the intestine. Regions in boxes are magnified in adjacent panels. Scale bars represent 100 μm. "L" indicates the lumen of the colon, triangles denote the layer of epithelial cells, "S" indicates the region of submucosal tissue, and arrows denote the boundary between the mucosa and submucosa defined by the muscularis mucosae. (B) Changes in body weight were tracked over time and compared to initial measurements on day 0. (C) Mice were evaluated each day for observable symptoms of disease that included: weight loss, hunched posture, poorly groomed fur, the consistency of stool and the presence or absence of blood,

and the presence and size of rectal prolapse. (D) Blinded assessment of pathological tissue alterations included: degree of epithelial disruption, degree of immune infiltrate, degree and size of submucosal tissue swelling, hyperplasia/proliferation of the muscularis mucosae layer, and degree of vascular remodeling on day 7 of DSS treatment. (E) Colon length on day 7 of DSS as measured from the cecum to the rectal end of the colon. Data are reported as mean ± SEM; n = 4–8 mice per group. Statistical test: paired t-tests.

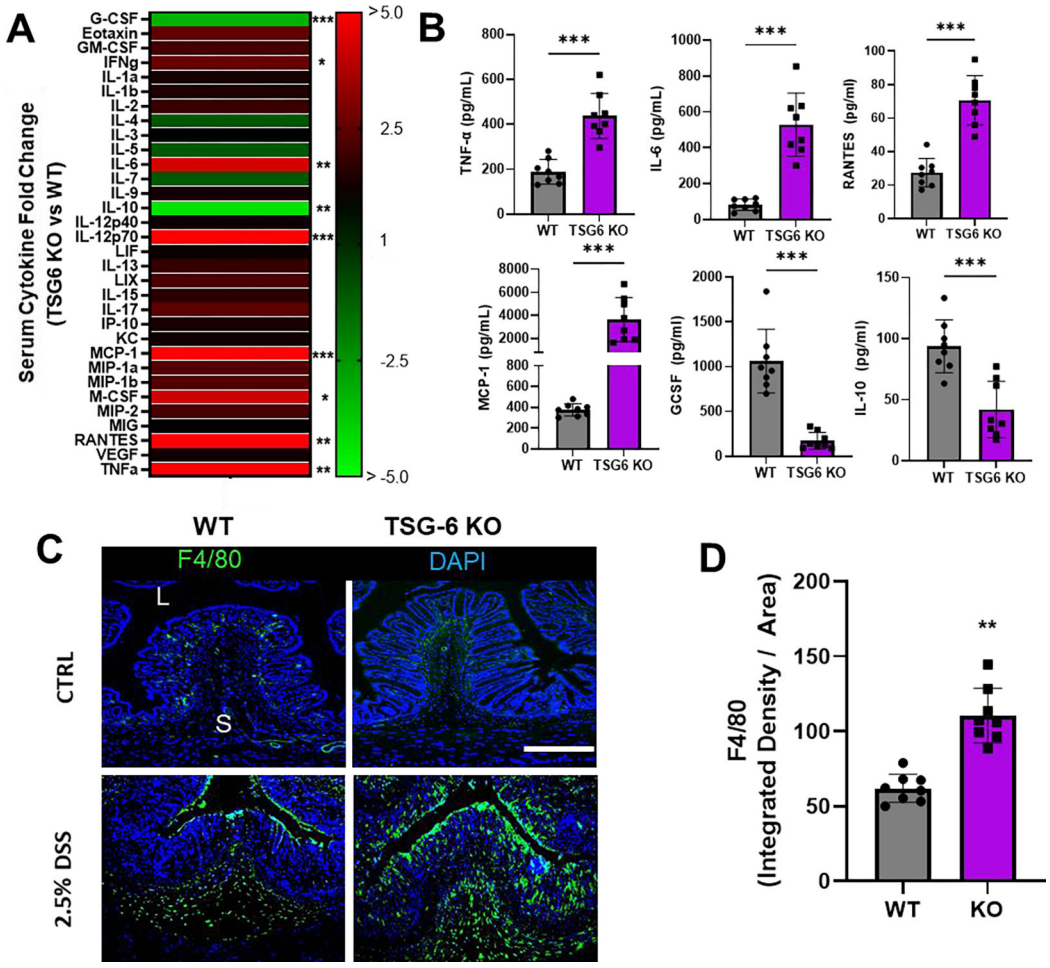

Figure 4. TSG6 deficiency leads to elevated levels of chemokines, cytokines, and macrophages on day 7 of DSS-colitis.

(A) Serum harvested on day 7 of colitic or control mice was analyzed for levels of 32 cytokine/chemokines by multiplex array. Cytokine levels are reported as fold change relative to WT. (B) Cytokine/chemokine levels in colon tissue were measured by ELISA. (C) F4/80+ macrophages were detected in colon tissue sections on day 7 of DSS by immunostaining with anti-F4/80 (green) and counterstained with DAPI for nuclei (blue). “L” denotes the lumen of the colon, “S” denotes submucosa. Images are representative of n=8 mice. (D) The mucosal area stained with F4/80 is quantified based on percent of total area analyzed and normalized against a secondary-reagent only control. Data are reported as mean ± SEM; n = 8 mice per group. Statistical test: paired t-tests. *P < .05; **P < .01; ***P < .001.

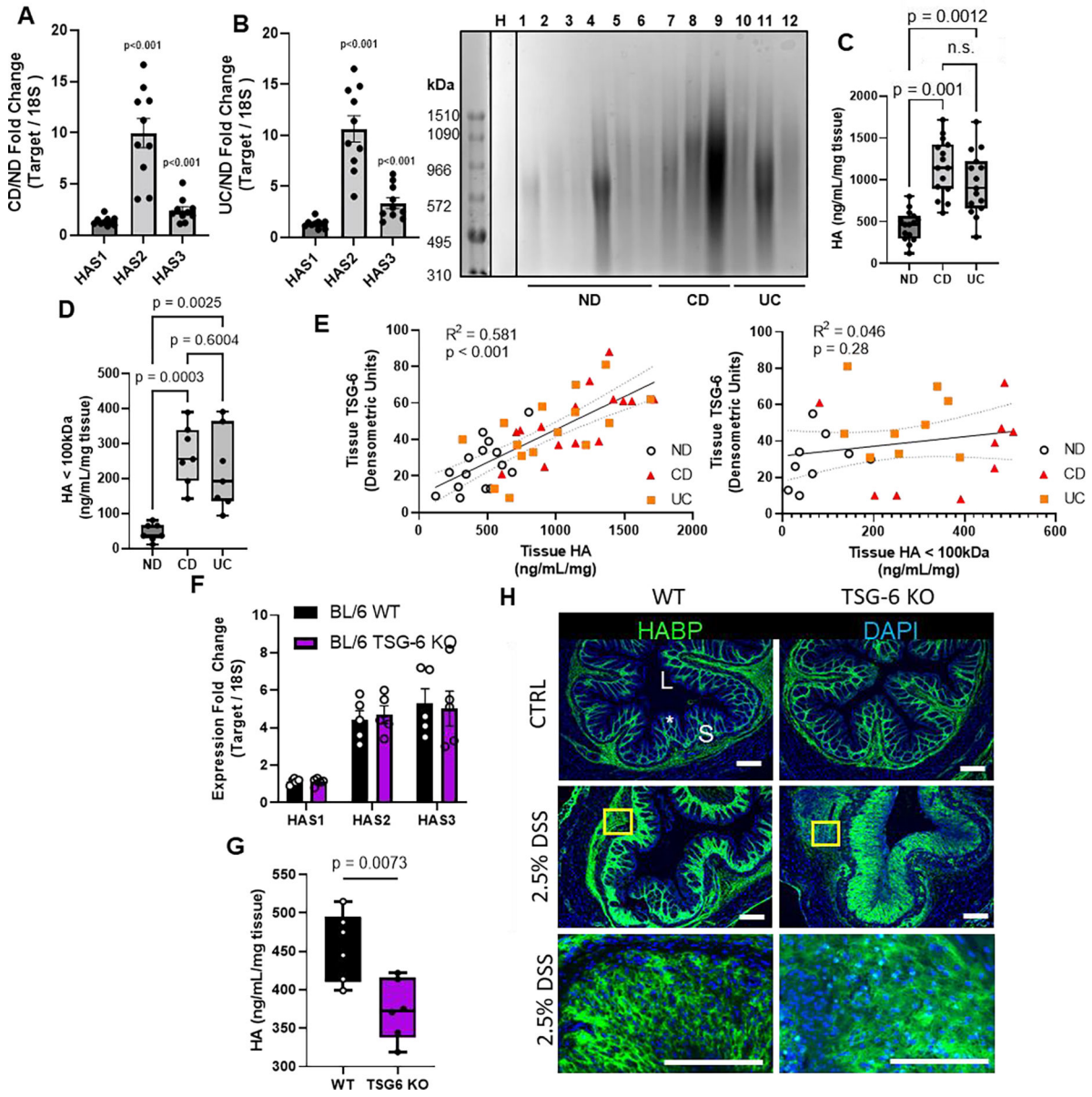

Figure 5. Characterization of tissue HA levels and organization in colitis.

Colon tissue lysates from non-IBD (ND), or IBD patients (n= 10 per group) with active colonic disease were homogenized and evaluated for (A) mRNA expression of HA-synthases (1–3) normalized to r18S, (B) HA size profile of HA purified from 6 ND and 6 IBD colon tissues. Predigestion of tissue isolate with Streptomyces hyaluronidase (H) is used as a specificity control, (C) total tissue HA levels and (D) low-molecular weight HA <100 kDa were quantified by ELISA-like assay. Linear regression analysis (E) comparing steady-state TSG6 protein and HA levels in patient colon tissue. Colon tissue from mice subject to 7 days of 2.5% DSS-induced colitis were measured for (F) mRNA expression of HA-synthases (1–3) normalized to r18S, (G) total tissue HA levels by ELISA-like assay, and (H) distal colon sections were evaluated for HA distribution by immunostaining for HA (green) and counterstained with DAPI (blue) for nuclei. “L” denotes the lumen, “*” denotes

mucosa, “S” denotes submucosa. Data are representative of at least 5 mice per group and are reported as mean ± SEM; Statistical test: paired t-tests, simple linear regression. Dotted lines indicate 95% CI. Imaging, detection, and software details: TCS SP5 II confocal/multiphoton high-speed upright microscope, HCX PL APO 40X/1.25NA oil immersion objective, HyD system detector, and LAS AF software (all Leica Biosystems) Scale bars indicate 100 μm.

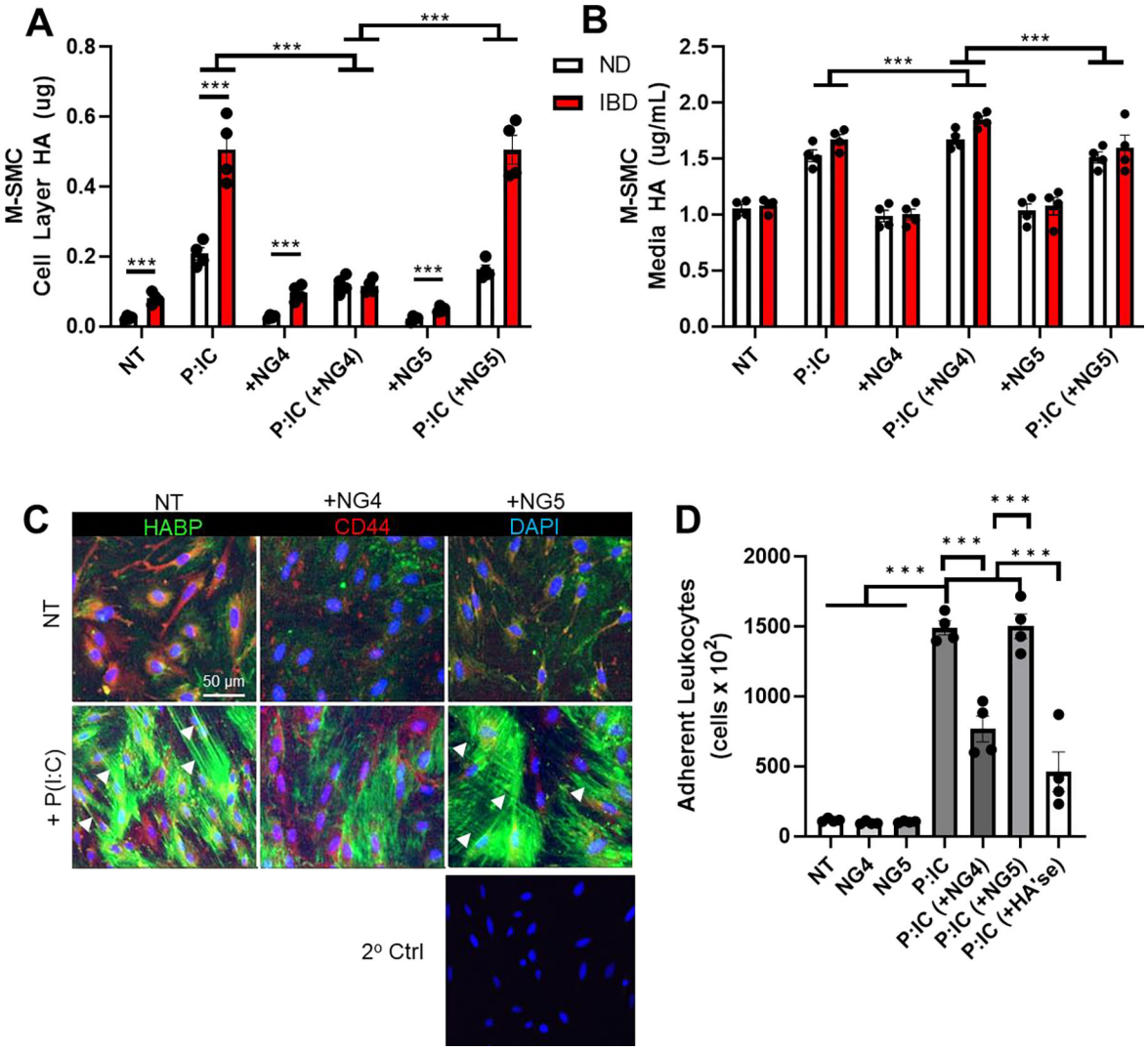

Figure 6. Antibody inhibition of TSG6 HC-transferase activity alters cell surface HA and leukocyte adhesion.

Confluent M-SMCs derived from either non-IBD or IBD patients were incubated with control media or stimulated with poly(I:C) (100 μg/ml) for 18 hours in the presence or absence of mAbs NG4 or NG5 (500ng/mL). HA attached to the cell layer (A) or released into media (B) was measured by ELISA-like assay. (C) Cell-surface HA was observed by immunohistochemistry using a specific HA-binding probe (HABP, green), and the M-SMC membrane was detected using a monoclonal antibody to the HA receptor CD44 (red). Nuclei were detected with DAPI (blue). Under basal conditions, HA on the surface of M-SMCs is present as a pericellular coat, while poly(I:C)-stimulated cells demonstrate HA organized into long “cables” (arrows) and an expanded pericellular HA matrix. In cells treated with the TSG6-inhibitory mAb NG4 (500ng/mL) HA cables are not present, while pericellular HA appears intact. Whereas cells treated with mAb NG5 (500 ng/mL) which binds but does not inhibit TSG6 still possess HC:HA cable structures. Cells incubated with secondary detection reagents alone are shown as a specificity control (2° Ctrl) Scale bar = 50 μm.

(D) M-SMCs were treated as above prior to the addition of Calcein AM-labeled PBMCs (1×10^6 cells/mL) and adherent PBMC were counted described in Materials and Methods. Prior to measuring adhesion, a replicate set of cells was also treated with hyaluronidase (HA'se, 100 mU/mL) as a control for HA-dependent adhesion. Data are representative of at least 4 independent experiments and are reported as mean ± SEM; Differences between multiple groups were calculated using 1-way ANOVA (Kruskal-Wallis test) with Dunn's correction for multiple comparisons. * $P < .05$, ** $P < .01$, *** $P < .001$.

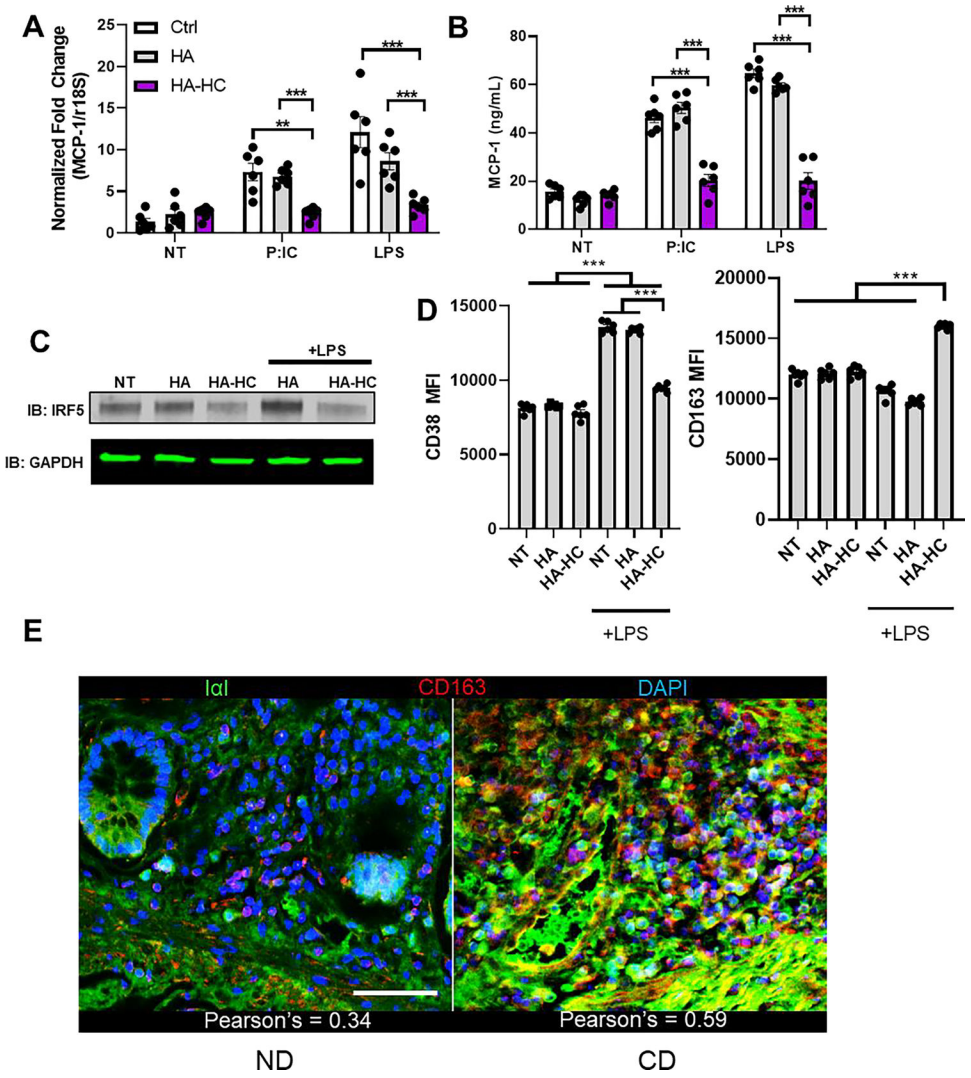

Figure 7. Interaction of activated monocytes with HC:HA alters the inflammatory response.

U937 monocytes (1×10^5) were cultured in the presence or absence of Poly(I:C) (100 μg/ml) or LPS (1 μg/ml) on immobilized control (Ctrl), HA, or HC:HA for 4 hours (qPCR) or 18 hours (ELISA) at 37 °C. (A) mRNA expression levels of MCP-1 normalized to r18S, (B) levels of MCP-1 secreted into in the conditioned medium as measured by ELISA. (C) IRF5 was detected by western blot in monocytes cultured for 18 hours and normalized by GAPDH. (D) Quantification of Mean Fluorescence Intensity (MFI) of CD11b+ U937 monocytes expressed as MFI of positive cells stained for surface CD38 and CD163 after 18 hours of culture in the presence or absence of LPS on immobilized control, HA, or HC:HA was measured by flow cytometry. (E) Human colon tissue sections immunostained for HCs of IαI (green) M2 marker CD163 (red) and dapi (blue). Images shown are representative of other replicates from different CD and UC patients with active IBD. Data are representative of at least 4 independent experiments and are reported as mean ± SEM; Differences between multiple groups were calculated using 1-way ANOVA (Kruskal-Wallis test) with Dunn's correction for multiple comparisons. * $P < .05$, ** $P < .01$, *** $P < .001$. Pearson's correlation coefficients were obtained by analyzing individual images (layers) of the Z-stack

using Image-Pro Plus software (Media Cybernetics, Rockville, MD). Imaging, detection, and software details: TCS SP5 II confocal/multiphoton high-speed upright microscope, HCX PL APO 40X/1.25NA oil immersion objective, HyD system detector, and LAS AF software (all Leica Biosystems) Scale bar = 100 μm.

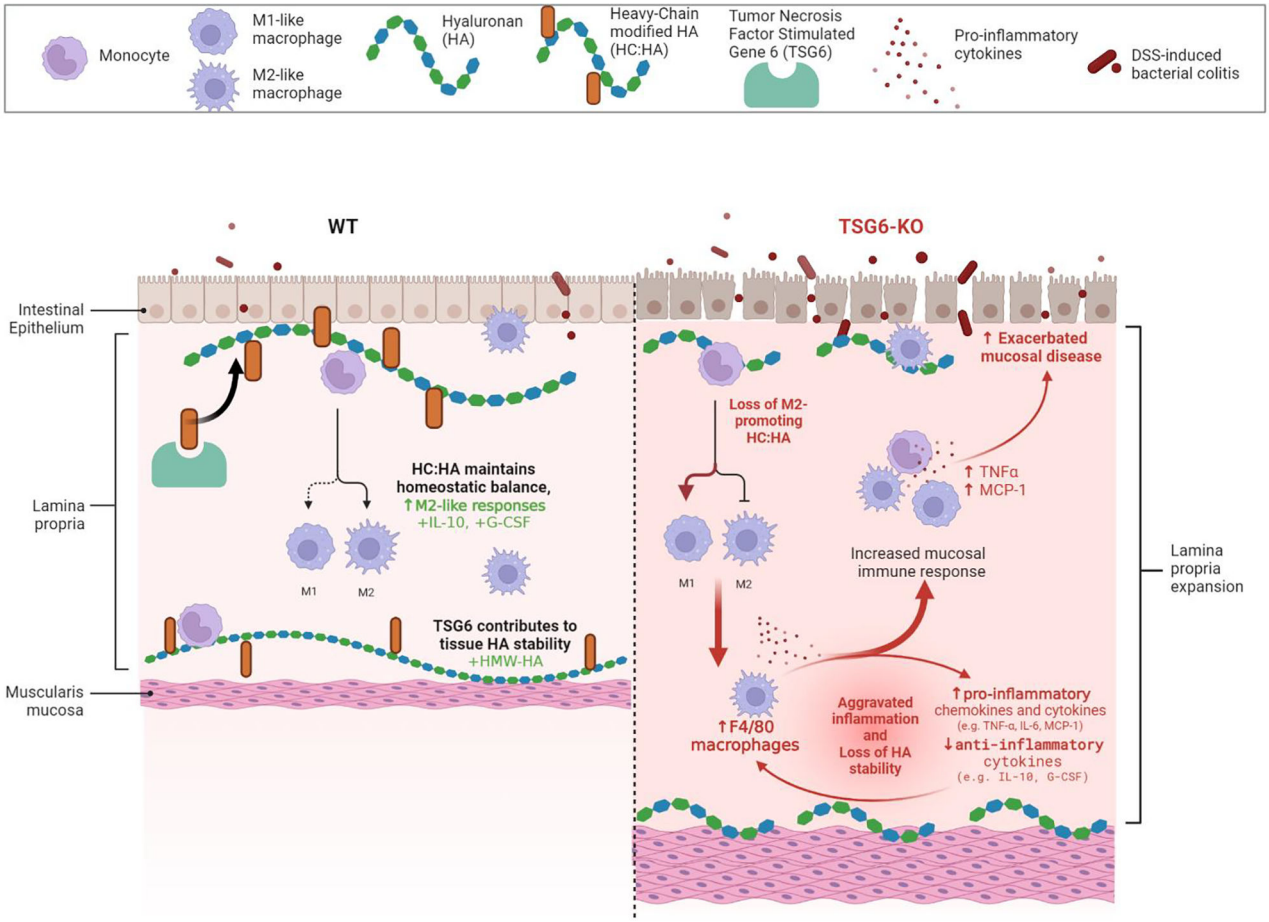

Figure 8. Proposed mechanism by which TSG6 generation of HC:HA matrices contributes to immune- and extracellular matrix-homeostasis in the intestine.

Our data from humans and mice suggests that TSG6-dependent generation of HC:HA matrices contributes to immune homeostasis by supporting M2-like responses while also contributing to the size, quantity, and stability of tissue HA levels during inflammation.

Table 1.

Characteristics of IBD Patient Cohort

Column1	Patient Characteristics	Control non-IBD (n = 15)	Ulcerative Coitis (n = 17)	Crohn's Disease (n = 17)
Demographics	% Male	48%	53%	60%
	Age			
	18–40	52%	53%	50%
	40+	48%	47%	50%
	African American, Hispanic, Asian, Native American, Pacific Islander	10%	10%	10%
Disease Characteristics	Years since diagnosis Mean (SD)	-	6.7 (8.2)	6.6 (9.3)
	Location of Disease	-		
	Ascending or Transverse Colon	-	47%	50%
	Descending or Sigmoid Colon	-	11%	10%
	Rectum	-	11%	10%
	Multiple Disease regions	-	30%	30%